

bradscholars

Förster Resonance Energy Transfer across interpolymer complexes of poly(acrylic acid) and poly(acrylamide)

Item Type	Article
Authors	Swift, Thomas;Paul, N.;Swanson, L.;Katsikogianni, Maria;Rimmer, Stephen
Citation	Swift T, Paul N, Swanson L et al (2017) Förster Resonance Energy Transfer across interpolymer complexes of poly(acrylic acid) and poly(acrylamide). Polymer. 123: 10-20.
DOI	https://doi.org/10.1016/j.polymer.2017.06.069
Rights	© 2017 Elsevier. Reproduced in accordance with the publisher's self-archiving policy. This manuscript version is made available under the CC-BY-NC-ND 4.0 license.
Download date	2025-04-22 06:16:02
Link to Item	http://hdl.handle.net/10454/12700

The University of Bradford Institutional Repository

<http://bradscholars.brad.ac.uk>

This work is made available online in accordance with publisher policies. Please refer to the repository record for this item and our Policy Document available from the repository home page for further information.

To see the final version of this work please visit the publisher's website. Access to the published online version may require a subscription.

Link to main paper: <http://hdl.handle.net/10454/12700>

Citation: Supplementary information for: Swift T, Paul N, Swanson L et al (2017) Förster Resonance Energy Transfer across interpolymer complexes of poly(acrylic acid) and poly(acrylamide). *Polymer*. 123: 10-20.

Copyright statement: © 2017 Elsevier. Reproduced in accordance with the publisher's self-archiving policy. This manuscript version is made available under the [CC-BY-NC-ND 4.0 license](#)



Förster Resonance Energy Transfer Across Interpolymer Complexes

Thomas Swift,^{*} Natalie Paul, Linda Swanson, Maria Katsikogianni and Stephen Rimmer^{*}

Supporting Information

Contents

Supporting Information	1
Polymer Characterization	2
Diffusion NMR	3
¹³ C NMR	6
Jablonski Diagram	9
Calculating Molar Absorption Coefficients	10
Response of ACE / AMMA label to pH	13
pKa Calculations	14
Energy Lost in Fluorescence – Stokes Shift	33
Label Molar Mass Distribution	16
Turbidity of Solution	17
Particle Size Summary	18
Fitting Fluorescence Lifetimes	33
E_{DT} of Dual Labels along Polymer Chain	38
E_{DT} of Single Labels along Multiple Chains	39
E_{ST} of Single Labels Across Multiple Polymer Chains	41
Optical Microscopy	19
Full Details of Fig. 13 and 14	42
AFM Microscopy	19

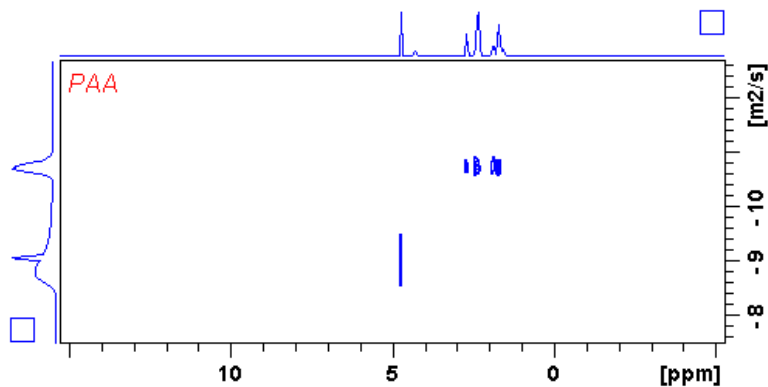
Polymer Characterization

Polyacrylamide samples were analysed at room temperature using a high molecular weight column setup consisting of 2x300mm TSKgell GMPWxl columns. All samples were run using aqueous solutions mobile phase of 0.1M sodium nitrate and 0.01 M sodium dihydrogen phosphate. Samples were prepared up to 1 mg ml⁻¹ and injected using a Rheodyne 200 um injection loop. The samples were analysed using a refractive index (RI) detector (HP 1047A RI Detector), calibrated to give polymer molecular weights calculated from the known retention time of standard PEG/PEO polymers.

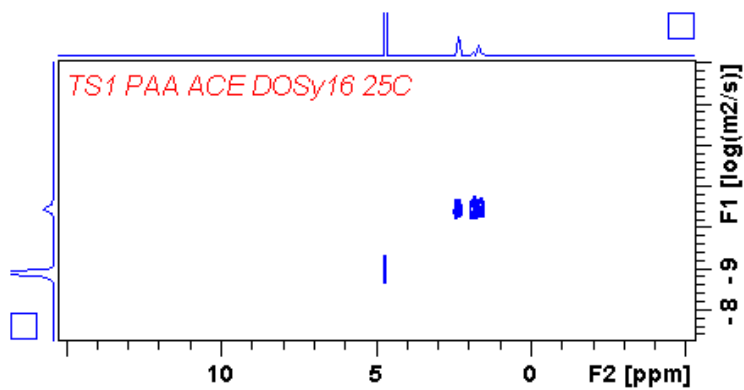
Acidic samples were modified via a methylation reaction with trimethylsilyldiazomethane. The product was then dissolved in THF (solvent filtered by 0.45 µm pore). A Kinesis 307 Gilson Pump passed the sample through 3x PLgel 10um mixed-B LS Columns at 1.00 ml/mn flow rate. Samples were added via a Anachem 234 auto injector and the RI signal was recorded using an Erma Inc. ERC-7512 RI detector. The system was calibrated using PMMA samples. A dual UV-RI system was used to determine that both naphthalene and anthracene labels were equally distributed through the entire molar mass distribution.

Diffusion NMR

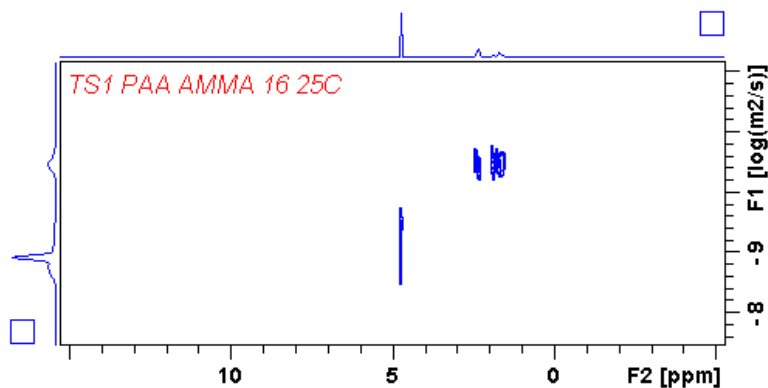
Raw diffusion data show PAA / PAM copolymers and D2O proton peaks along X axis, with distinct diffusion ($\log D$ data shown) peaks along the Y axis. As low loading of ACE and AMMA labels is present only the main polymer backbone is observable.



PAA
 $\log D = 10.75$
H₂O $\log D = 9.8$



PAA ACE
 $\log D = 10.50$
H₂O $\log D = 8.92$



PAA AMMA
 $\log D = 10.51$
H₂O $\log D = 8.96$

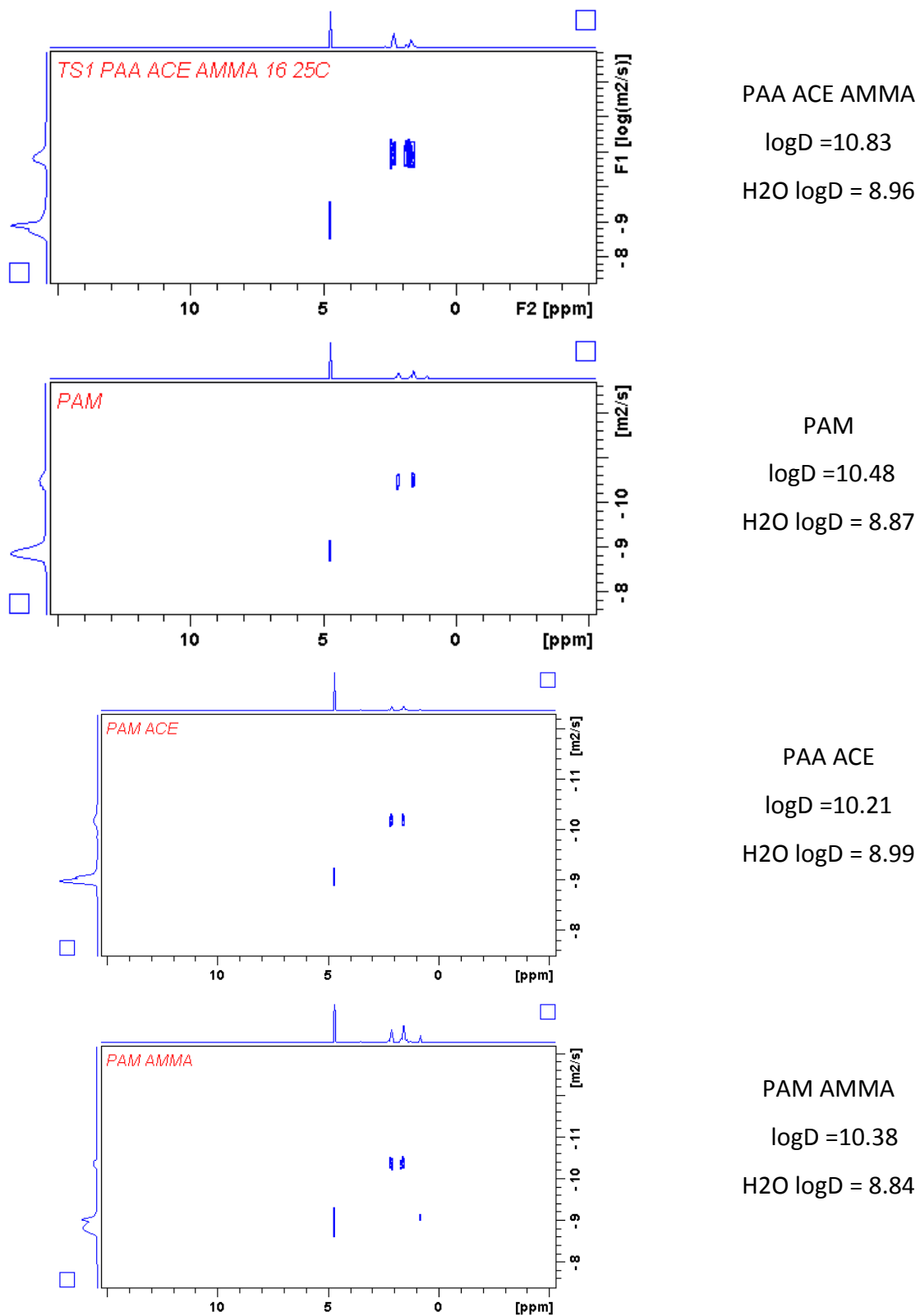


Fig. S1 – Diffusion NMR spectra of polymer samples

The conformational change of poly(acrylic acid-co-ACE) in solution can be measured using this technique. Reinterpretation of previously published diffusion data of RAFT produced PAA polymers¹ shows that poly(acrylic acid) and poly(acrylic acid-co-ACE) of similar molecular weights (52.5 and 55.9 kDa) have equivalent hydrodynamic radius and transitions (8-10 nm transitioning to 30-31 nm), inferring that the presence of the acenaphthylene has no effect on the macromolecular solution properties of the polymer (Fig. 4).

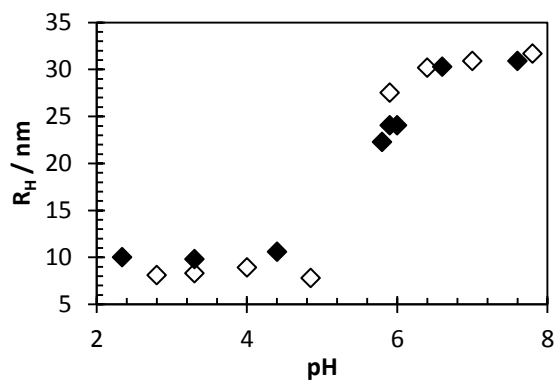


Figure S2. Hydrodynamic radius of poly(acrylic acid) (◆) and poly(acrylic acid-co-ACE) (◇) in D₂O spiked with low concentration NaOH / HCl to adjust pH.

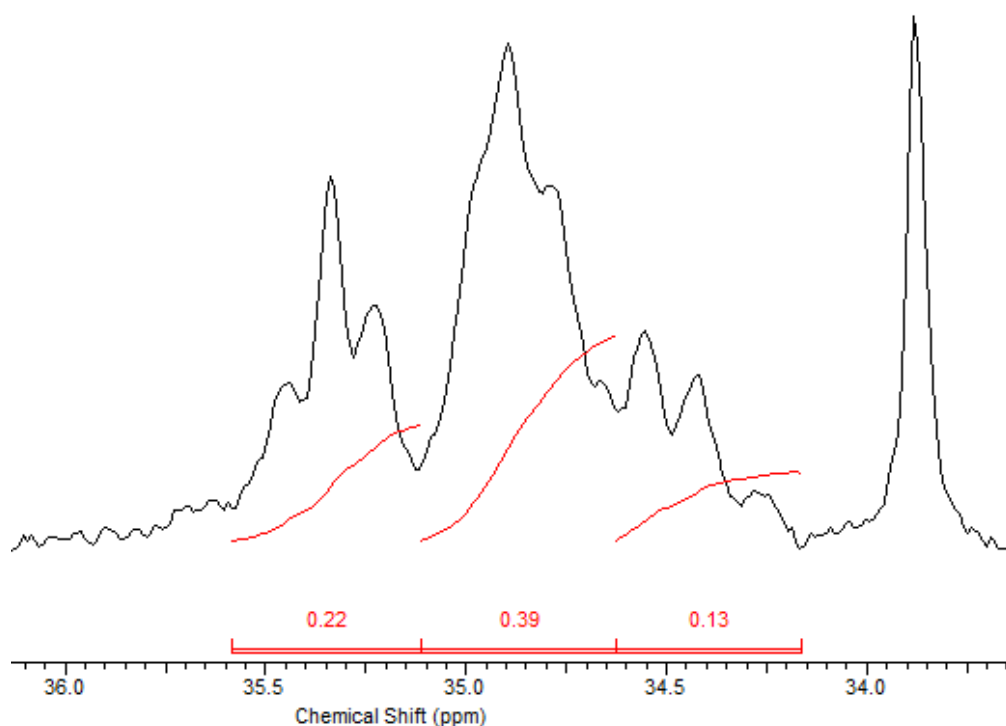
¹³C NMR

Tacticity of polymers was confirmed using the %syndiotactic and % isotactic peaks using the integrals of peaks that were found to derive from mm, mr and rr triads.

$$%I = \int mm + \frac{1}{2} \int mr$$

$$%S = \int rr + \frac{1}{2} \int mr$$

For this study the integrals of poly(acrylic acid) were taken corresponding to the backbone carbon with 36 – 35.2 ppm representing the rr triad (mrrm, mrrrr and rrrr pentads), 35.2 – 34.6 the mr triad (rmrm, rmrr, mrrm, mmrr pentads) and 34.6 – 34.2 the mm triad (rmmr, mmmr and mmmm pentads). These were found following previous work by Chang, but had all shifted downfield compared to his earlier experiments.²



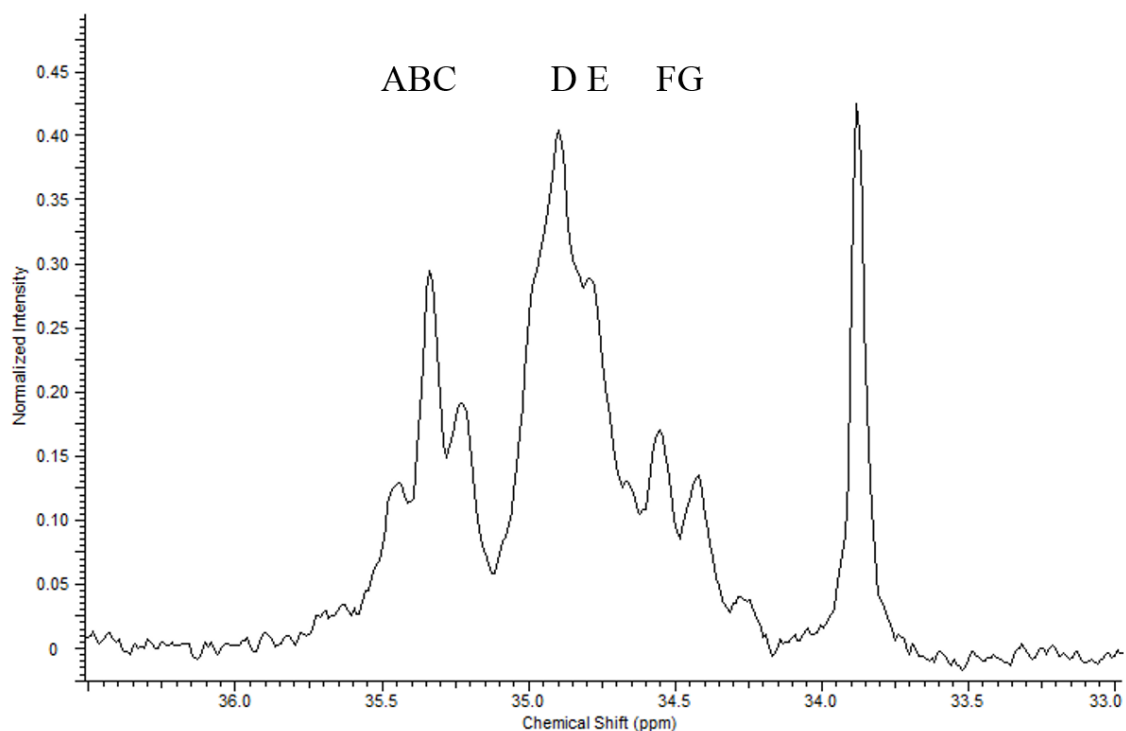


Fig S3 – Extracted ^{13}C NMR spectra of PAA (top – integrals, bottom - extracted peaks)

The data used to calculate these are shown below in Table S1. Raw data for these carbon nmrs is attached as a zip file with the supporting information. Data was analysed using ACD/2D NMR processor. Some samples gave poor baselines due to the extended length the samples had to be analysed to give observable signals of all peaks. This was dealt with by using a polynomial baseline to give spectra that could be cleanly integrated (Fig. S4).

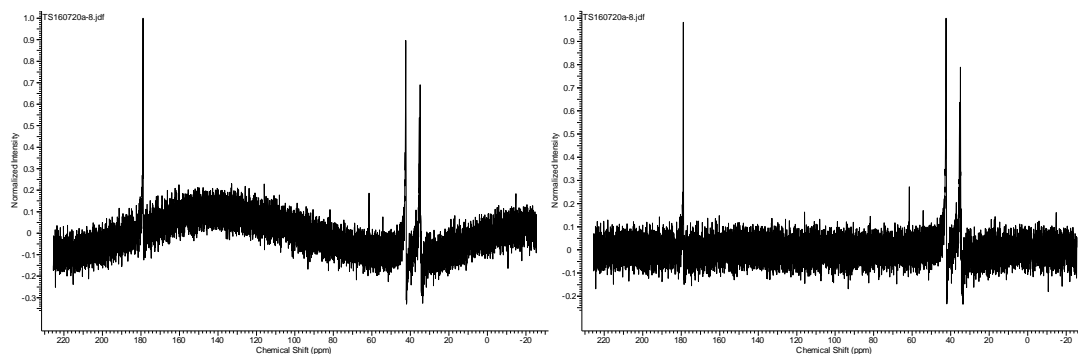


Figure S4 – Polynomial baseline fitting of P(AA-co-ACE-co-AMMA) to give flat baseline prior to integration of tacticity peaks.

Table S1. Raw data for ^{13}C integration used in Table 3.

Polymer	Triad	Integration	%
PAA	rr	0.22	30.5
	mr	0.36	50
	mm	0.14	19.4
PAA-ACE	rr	0.39	14.4
	mr	1.38	51.1
	mm	0.93	34.4
PAA-AMMA	rr	0.14	38.9
	mr	0.18	50.0
	mm	0.04	11.1
PAA-ACE-AMMA	rr	0.14	43.8
	mr	0.17	53.1
	mm	0.01	3.1
PAM	rr	0.11	34.4
	mr	0.17	53.1
	mm	0.04	12.5
PAM-ACE	rr	0.31	14.6
	Mr	1.05	49.5
	mm	0.76	35.8
PAM-AMMA	rr	0.15	7.3
	mr	1.18	57.3
	mm	0.73	35.4

Jablonski Diagram

Our two measurements (E_{ST} and $E_{D\tau}$) measure two different processes in the absorbance – fluorescence emission process of an excited state fluorophore. This can be explained using Fig. S5.

The first $E_{D\tau}$ shows the quenching of the donor excited state, as FRET occurs on a similar timescale to fluorescence (nanoseconds) both processes will compete resulting in a diminished fluorescence lifetime. Conversely E_{ST} reports on the total fluorescent output of both labels (F_D and F_A).

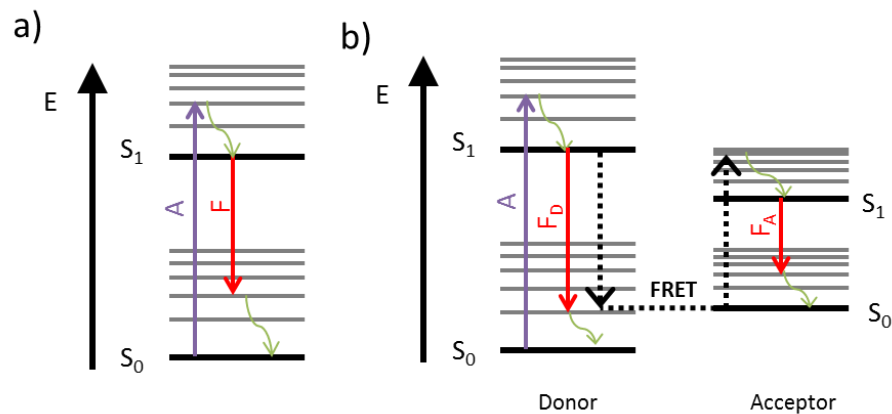


Figure S5. Jablonski diagram demonstrating energy states of a) typical fluorescence and b) FRET transfer of light between donor-acceptor labels of the chromophore excited state.

Calculating Molar Absorption Coefficients

The Beer-Lambert law ($A=\epsilon lc$) states that the absorbance of a label in fixed conditions (path length and solvent) is linear with concentration, as defined by the molar absorption (or extinction) coefficient (ϵ).

To determine the molar absorption coefficient, concentration gradients of acenaphthene and anthracene (substituted to better simulate the binding of ACE and AMMA to a polymer backbone (Figure S11)) were created in methanol, and analyzed to show relative absorbance (Figure S12 / S13).

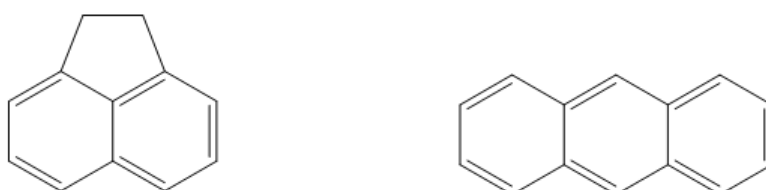


Figure S6 – Acenaphthene and Anthracene have identical aromatic structure to ACE and AMMA

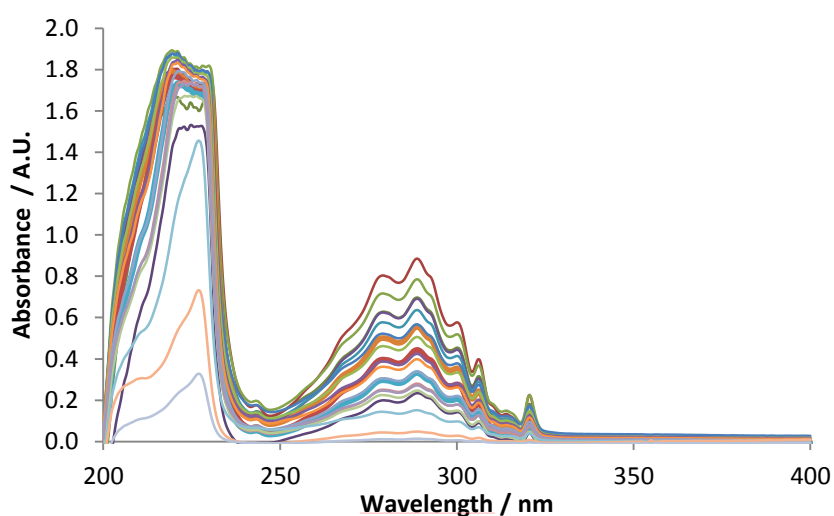


Figure S7 - Decreasing absorbance of acenaphthene peaks as concentration is reduced from 1E-4 to 5E-6 Molar

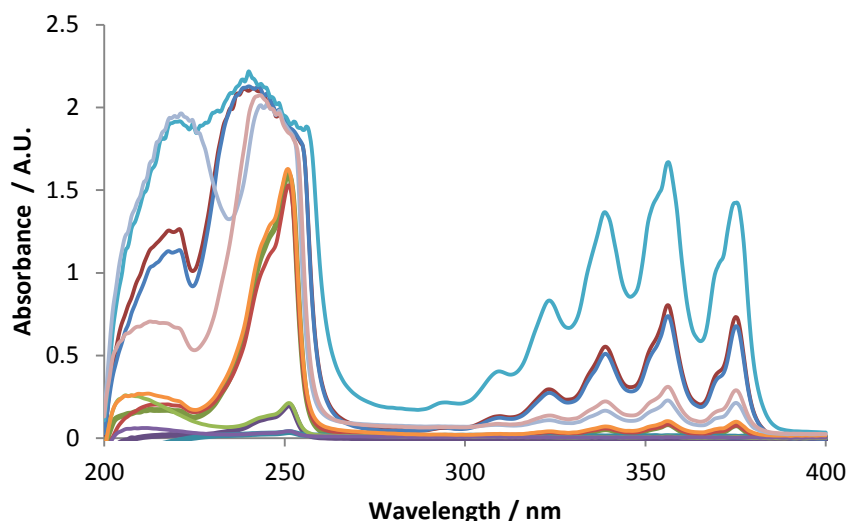


Figure S8 - Decreasing absorbance of anthracene peaks as concentration is reduced from 9E-4 to 1E-7 Molar

At low concentrations the correlation between the maximum peak absorbance (289 nm for acenaphthene / 256 nm for anthracene) and at low concentrations the relationship between concentration and absorbance is linear (Figure S5/ S6). From the gradient of the absorbance increase at low concentrations the molar absorption coefficients were calculated as $5699 \text{ mol}^{-1} \text{ cm}^{-1}$ for acenaphthene and $7202 \text{ mol}^{-1} \text{ cm}^{-1}$ for anthracene. This linear relationship breaks down at higher concentrations (approx. 0.0005 M for acenaphthene / 0.0002 M for anthracene) (Figure S7 / S8).

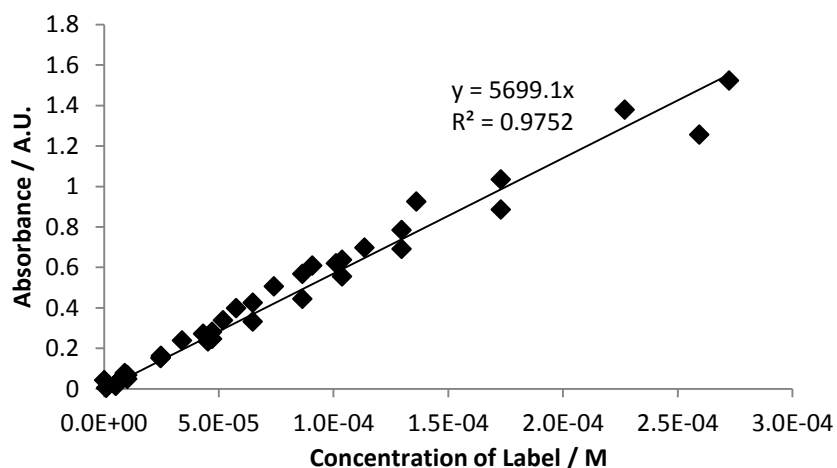


Figure S9 – Linear correlation of 289 nm peak of acenaphthene at low concentrations

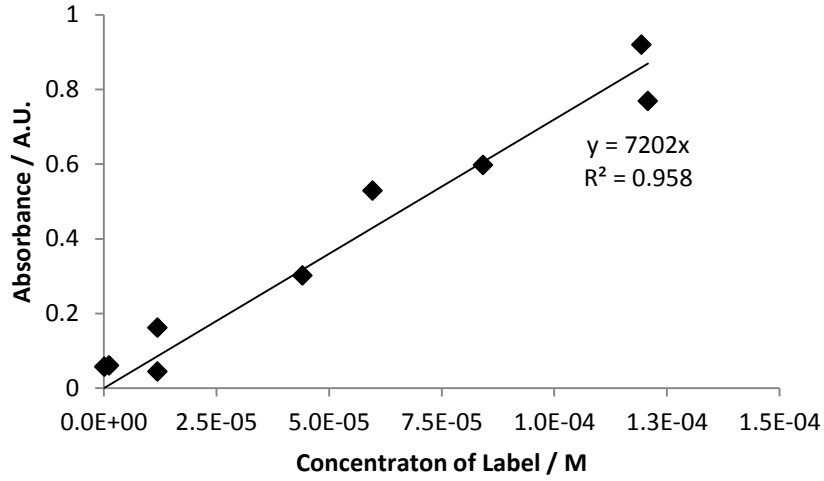


Figure S10 – Linear correlation of 289 nm peak of anthracene at low concentrations

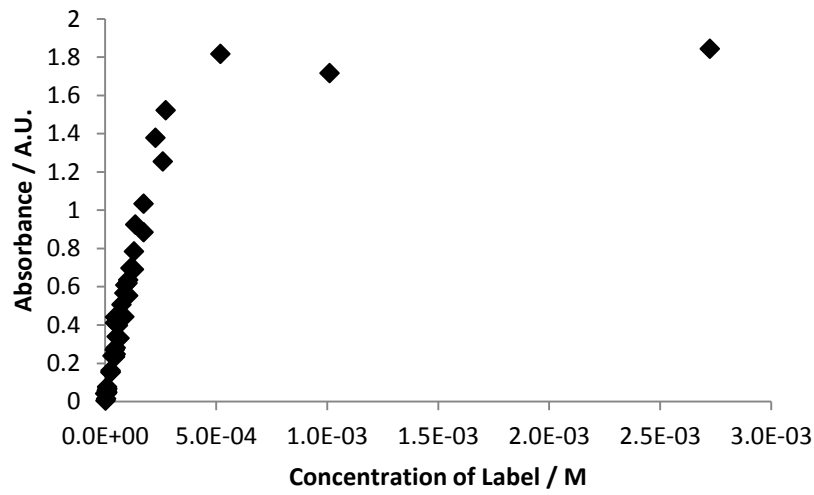


Figure S11 – Acenaphthene peak absorbances at 289 nm are no longer linear in concentrations exceeding 10^{-4} M

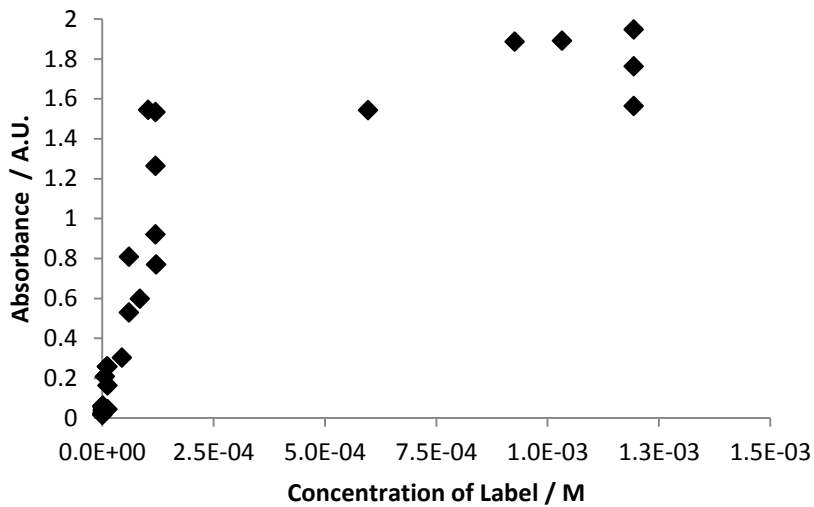


Figure S12 - Anthracene peak absorbance at 256 nm are no longer linear in concentrations exceeding $1E-4$ M

Response of ACE / AMMA label to pH

The emission and excitation spectrum of singly labelled PAA polymers do not alter significantly with the pH of the solution, although there is some slight quenching at higher pH (Figure S9). As the ACE-label is covalently bound to the polyacrylic acid chain the expansion/contraction of the polymer chain has no effect on the wavelengths or intensity of the label's luminescence. The AMMA label, bound pendent to the PAA chain, is slightly more sensitive to pH, although it retains similar structure and retains the same peak emission/excitation wavelengths (Figure S10).

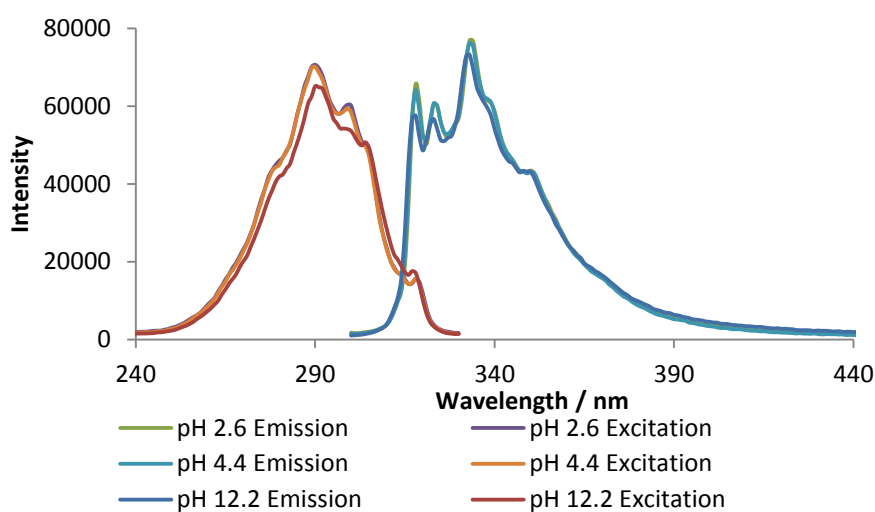


Figure S13 -- Emission/Excitation intensities of ACE-Labelled PAA polymers varying with pH

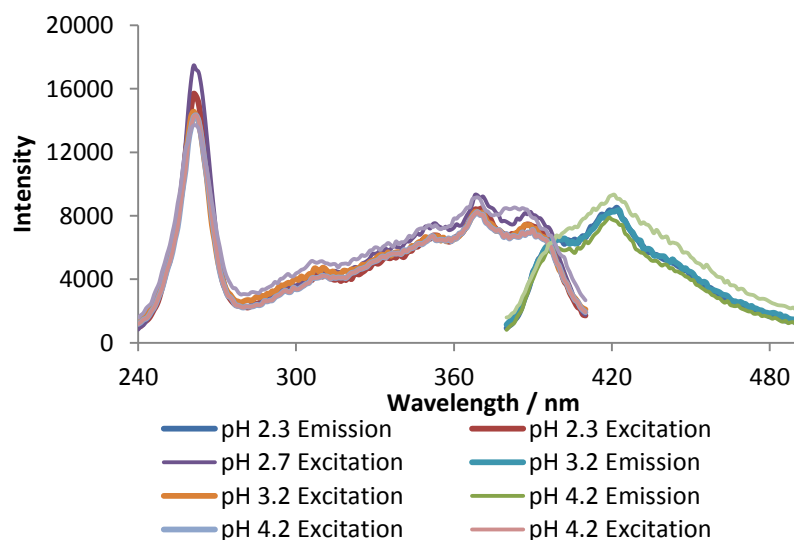


Figure S14 - Emission/Excitation intensities of AMMA-Labelled PAA polymers varying with pH

pKa Calculations

The pKa of acid polymers was determined via repeated titration ($n = 3$) via a Metrohm Titrino autotitrator, adding 0.01 M NaOH to 10 ml solutions of 0.01 M NaCl and 0.001 M HCl containing 10 mg polymer sample. The pKa was determined from automatically identified equivalence points via the Henderson Hasselbalch equation. The particle size of the polymers was measured using a Malvern Zetasizer Nanoseries Nano-ZS operating at a dual angle system. A dilute (1 mg ml^{-1}) solution of polymer in ultrapure water was loaded in a 10 mm path length cuvette and studied at $25 \text{ }^\circ\text{C}$. Dissolved polymer samples were filtered prior to mixing. Each sample was measured several times over multiple runs with a measurement time of 10s per run and the particle size determined by volume averaging using Zetasizer software. Comparison between samples was carried out using analysis of variance with a Tukey *post hoc* analysis.

The pKa was calculated via the Henderson – hasselbalch equation using the equivalence point from an acid-base titration. Each titration was performed in triplicate and the average pKa are shown below:

Sample	average pka	S.D.
PAA	4.54	0.04
P(AA-co-ACE)	4.53	0.09
P(AA-co-AMMA)	4.55	0.06
P(AA-co-ACE-co-AMMA)	4.50	0.07

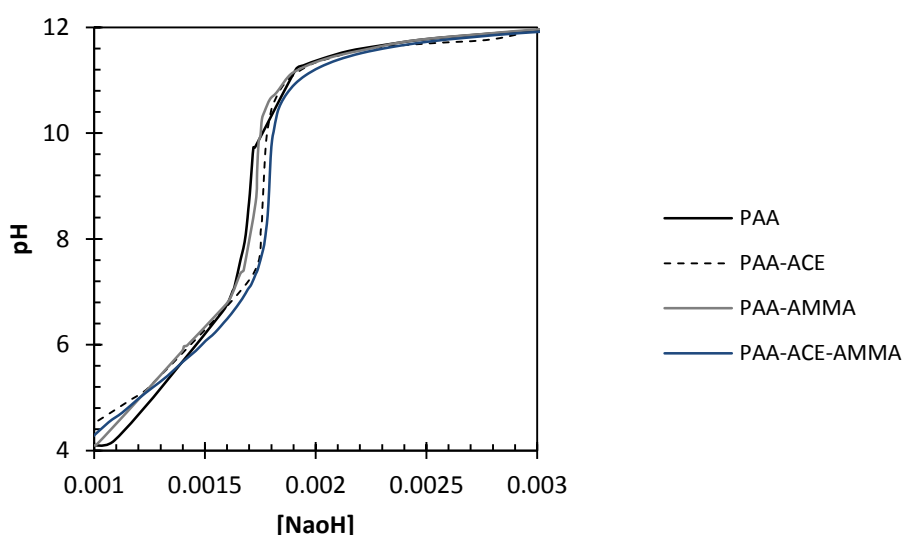


Figure S15 – PH titration of low molar mass polymer concentrations.

Label Molar Mass Distribution

Coupling a UV absorbance detector to SEC molar mass determination by RI it was shown that both fluorophores ACE and AMMA were equally distributed through polymer molar mass distributions.

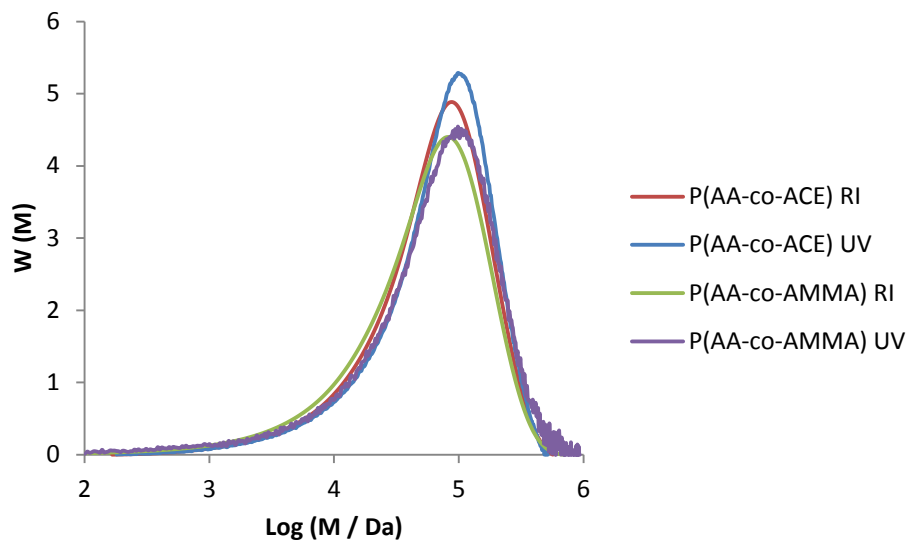


Figure S20 – Molecular Weight Distribution of P(AA-co-ACE) and P(AA-co-AMMA) (TS1/37/2) polymers

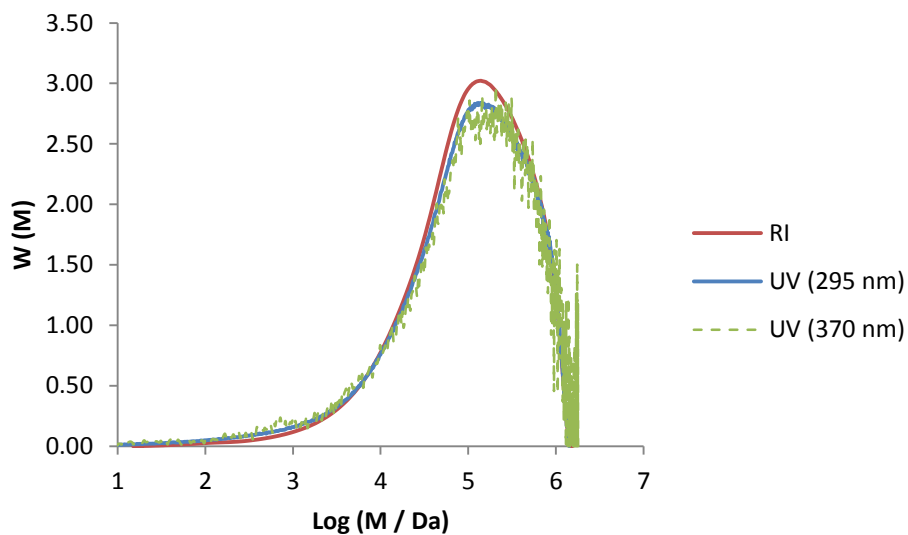


Figure S21 – Molecular weight distribution of P(AA-co-ACE-co-AMMA), showing ACE (UV 295 nm) and AMMA (UV 370 nm) distribution

Turbidity of Solution

Interpolymer complexation at high pH can also be measured by turbidity and the pH of the solution is critical for driving complexation. To re-enforce fluorescence evidence of the complexation the turbidity of solution was used to inform the presence / absence of complexation. Turbidity was estimated as a visual inspection of cloudy / not cloudy rather than using a turbidimeter.

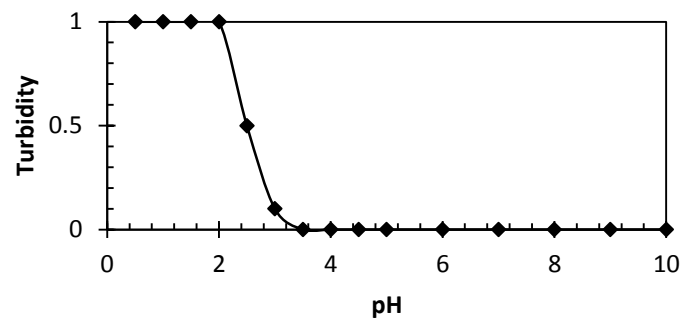


Fig. S22 – Turbidity (cloudiness) of a 5 mg ml⁻¹ concentration PAA + PAM



Fig. S23 – Turbidity (cloudiness) of PAA + PAM at pH 2 (left) and 7 (right) at 0.2 mg ml⁻¹

Particle Size Summary

Calculated particle sizes (diameter, nm) from light scattering experiment data shown in Fig. S24 and Table S2.

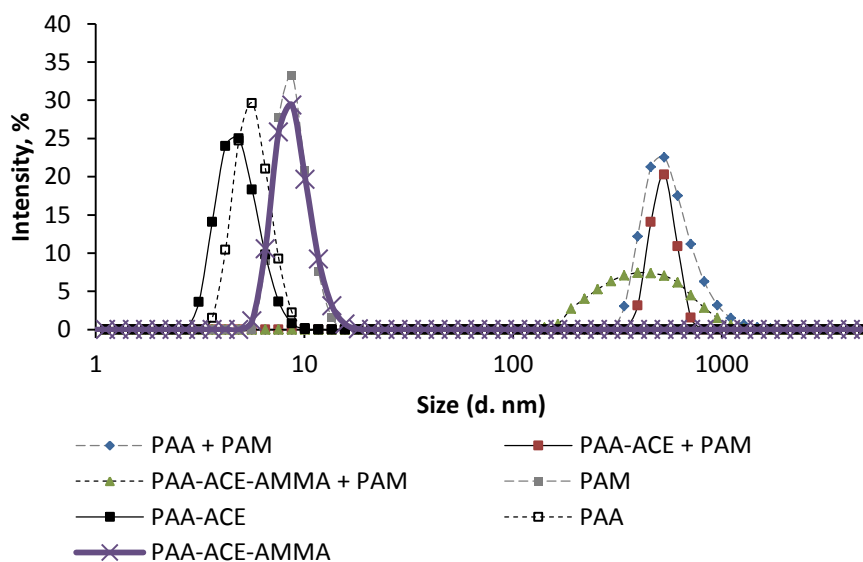


Fig. S24 - Particle diameter distributions of PAA (black markers), P(AA-co-ACE) (grayfilled markers) and/or P(AA-co-ACE-co-AMMA) (white markers) alone and mixed with equal conc (1 mg ml^{-1}) PAM.

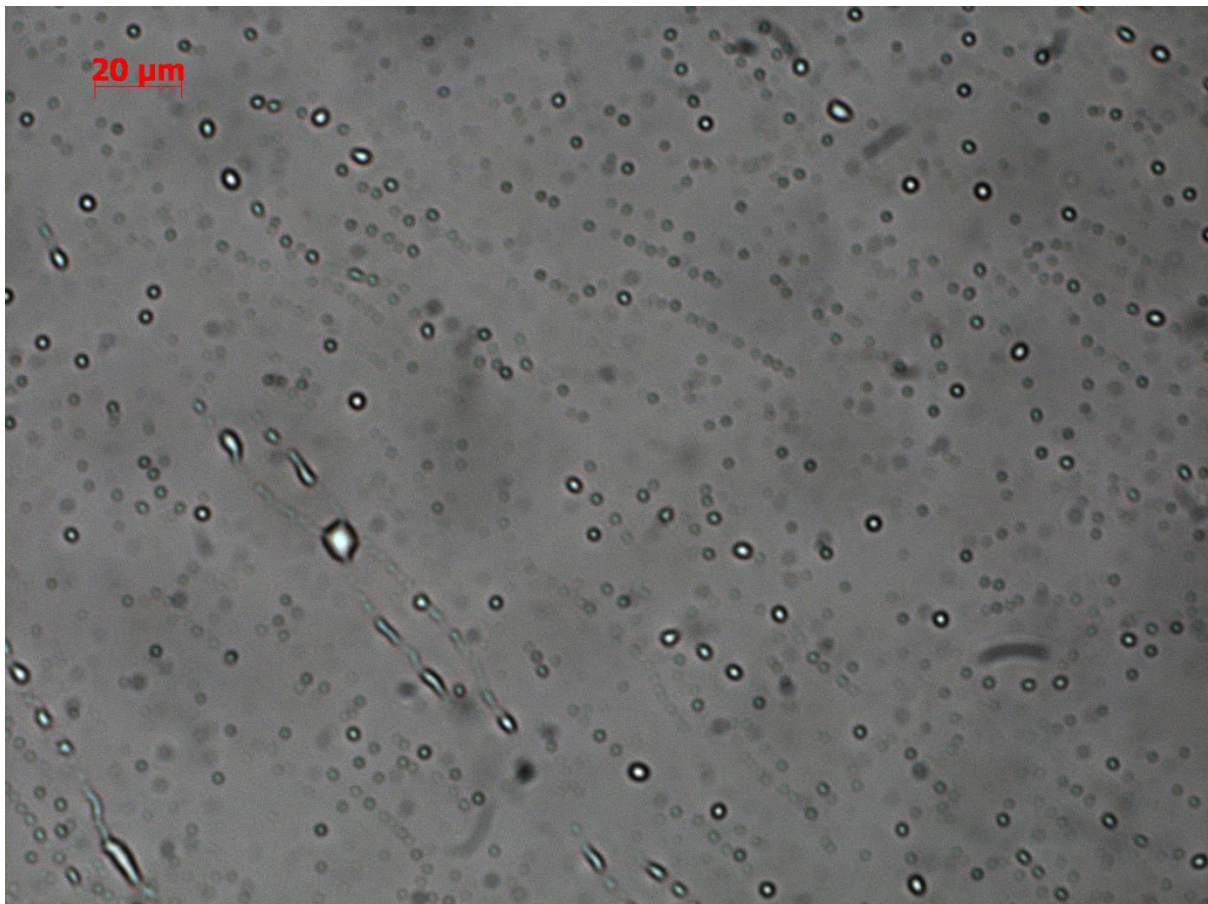
Table S2 – Average particle diameters and standard distributions of particles as shown in Fig. 4.

	PAA		PAA-ACE		PAA-ACE-AMMA		PAM	
	Mean	SD	Mean	SD	Mean	SD	Mean	SD
Polymer	7.692	3.054	6.858	1.025	8.762	1.609	8.716	3.438
Polymer + PAM	531.2	31.39	529.8	74.2	483	178.7	-	-

Optical Microscopy

Pictures were taken at pH 2 and 7 of the same 1 mg ml⁻¹ PAA-PAM solution dissolved in 0.001 M HCl and then mixed with 0.01 M NaOH to raise the pH. Full sized resolutions of images shown in the pictures are attached below.

pH 2:



Ph 7:

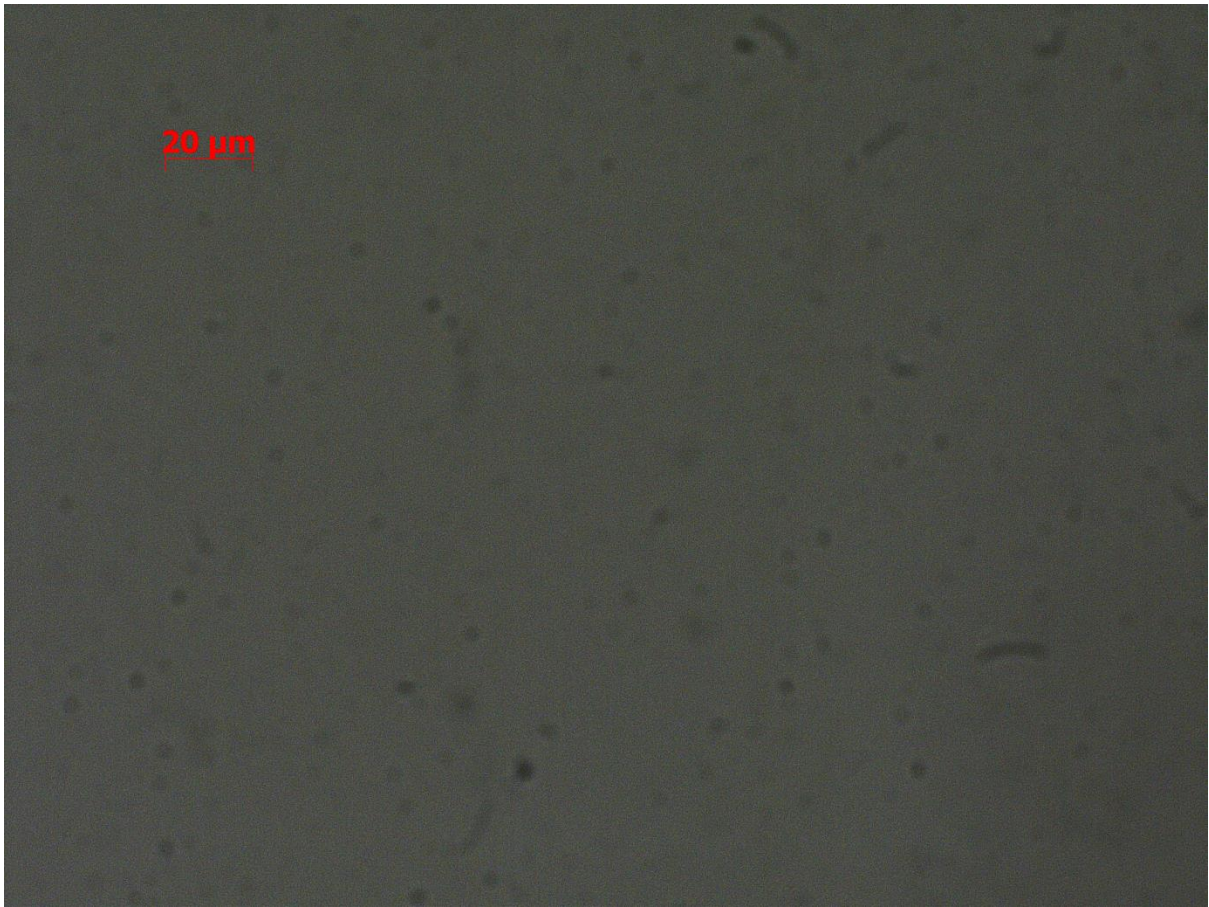


Fig S.29 – Optical Microscope images of polymer mixtures on glass slide.

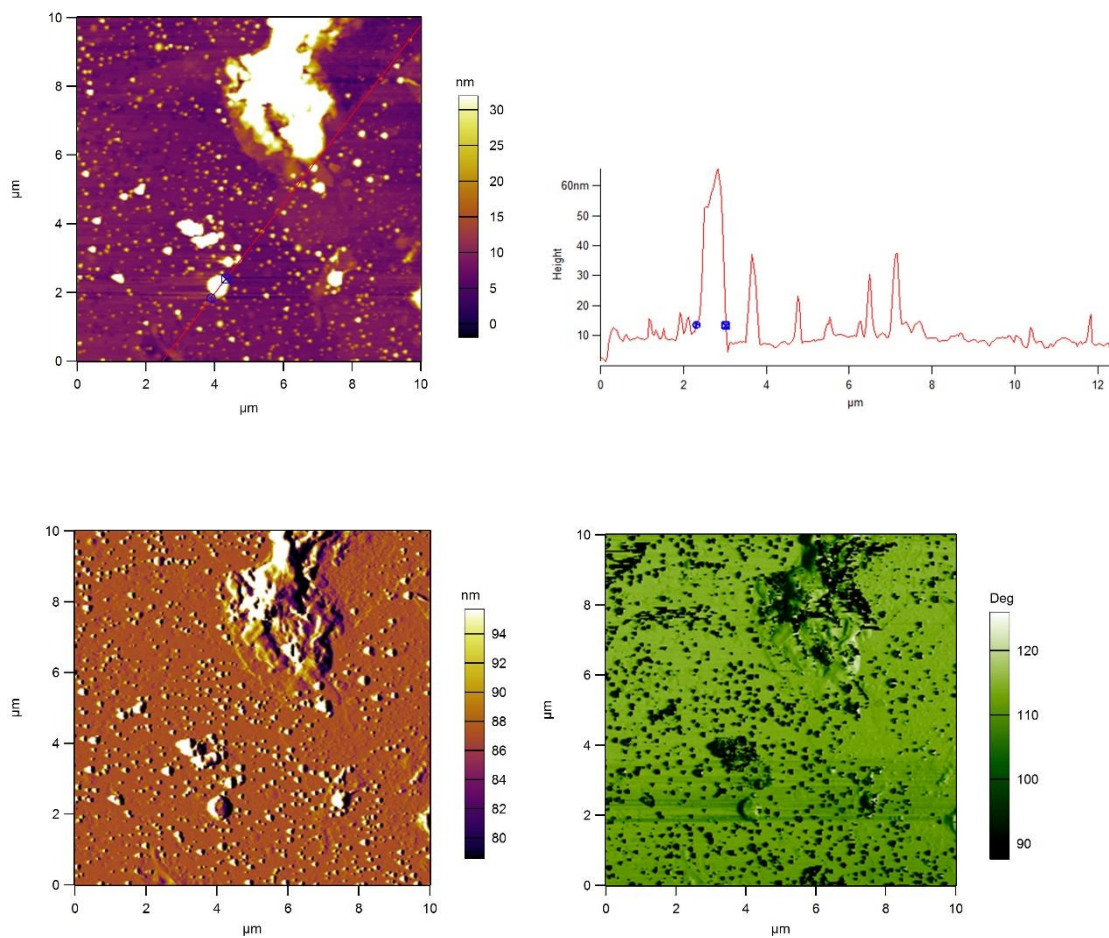
Atomic Force Microscopy

Typical AFM images of the samples are shown in the following Figures. Pictures are shown as height (top left), amplitude (bottom left) and phase (bottom right) distributions. Attempts to determine particle height profile along a crossline section in the height map are shown in the top right.

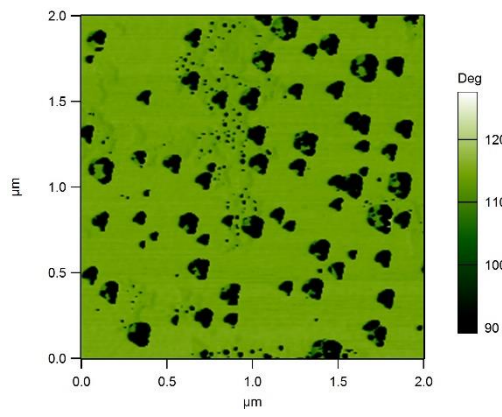
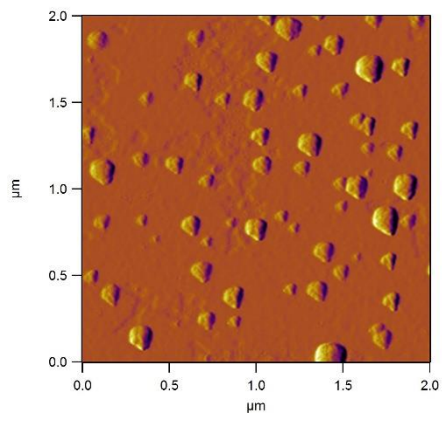
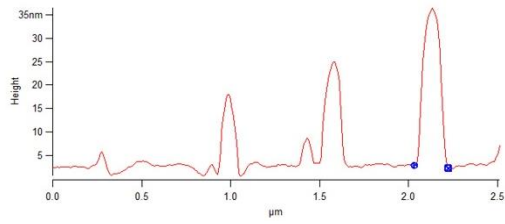
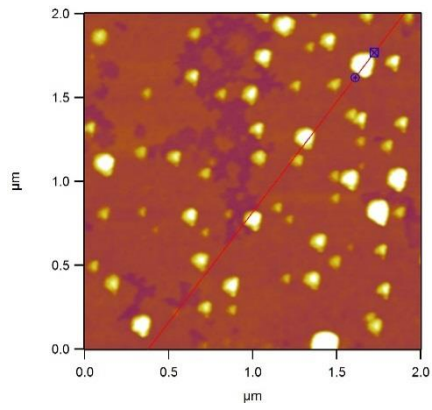
Sample A

(Complex of PAA-PAM at pH 2 – 0.05 mg ml⁻¹ component concentration)

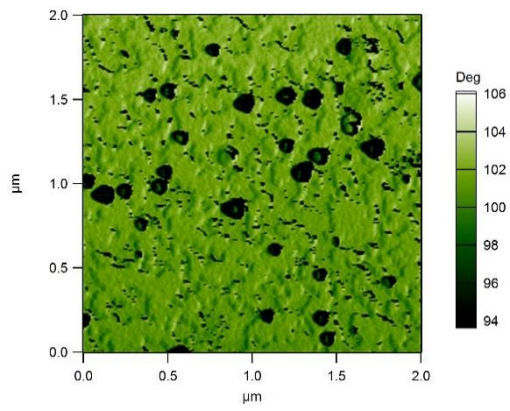
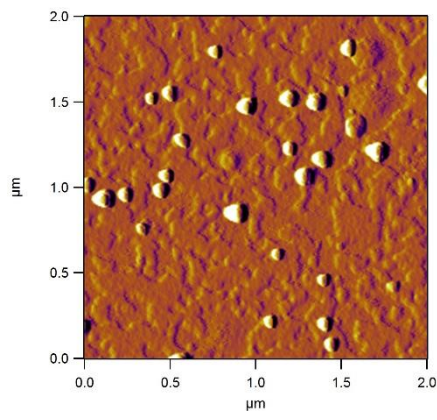
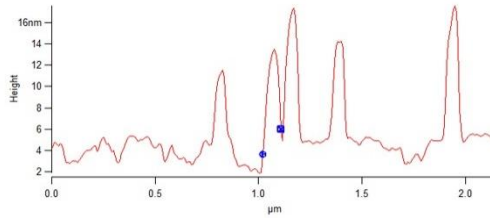
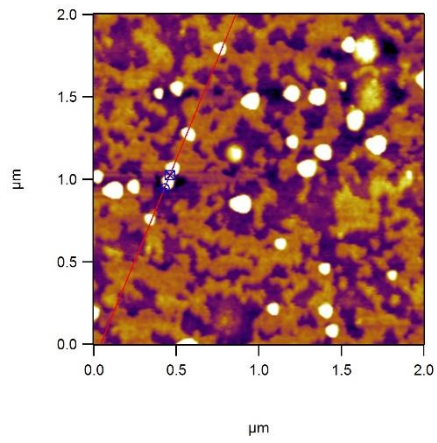
A20000: Height distribution: 8.5±1.2 nm



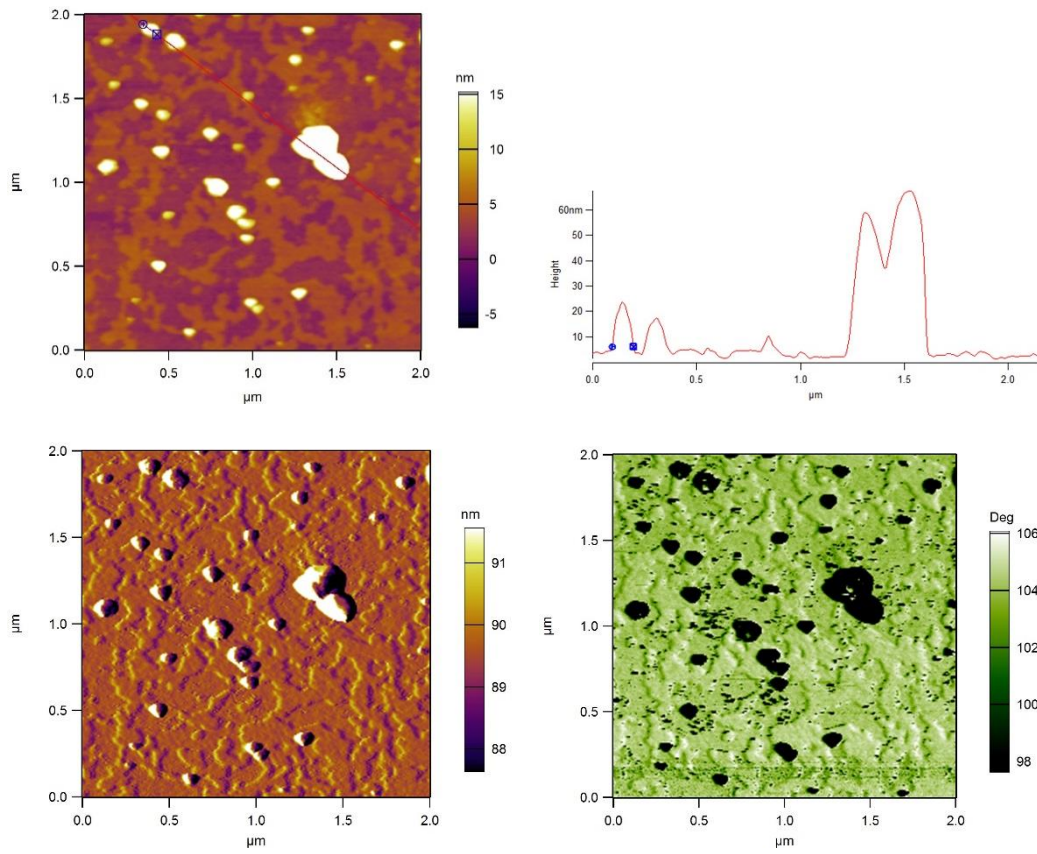
A20001: Height distribution: 2.88 ± 0.34 nm



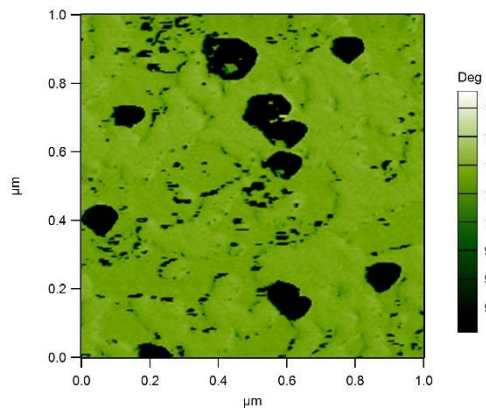
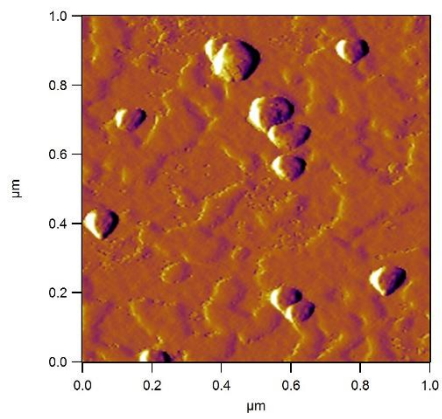
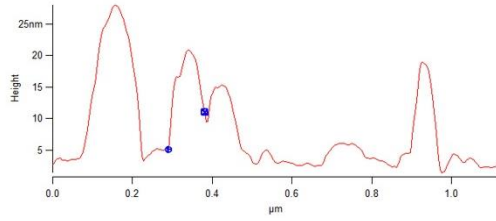
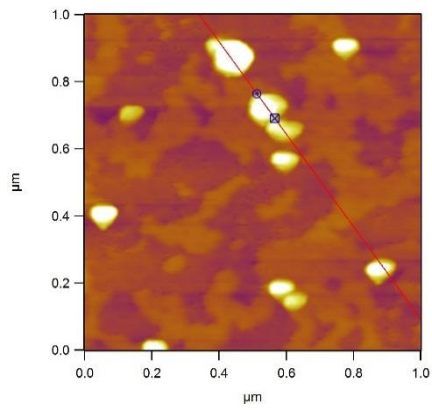
A20014: Height distribution: 4.05 ± 1.31 nm



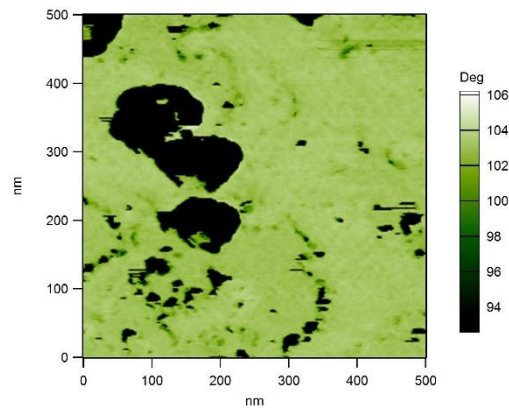
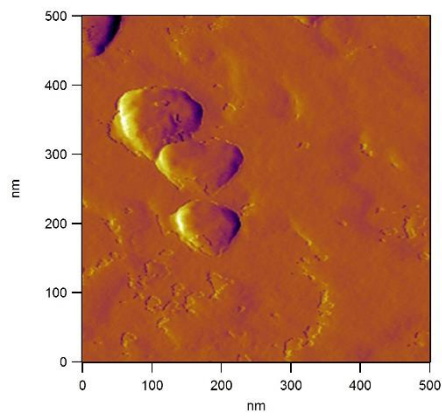
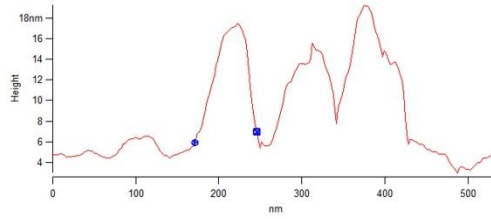
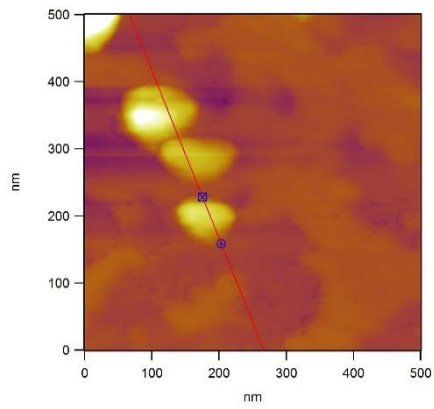
A20016: Height distribution: 3.28 ± 1.35 nm



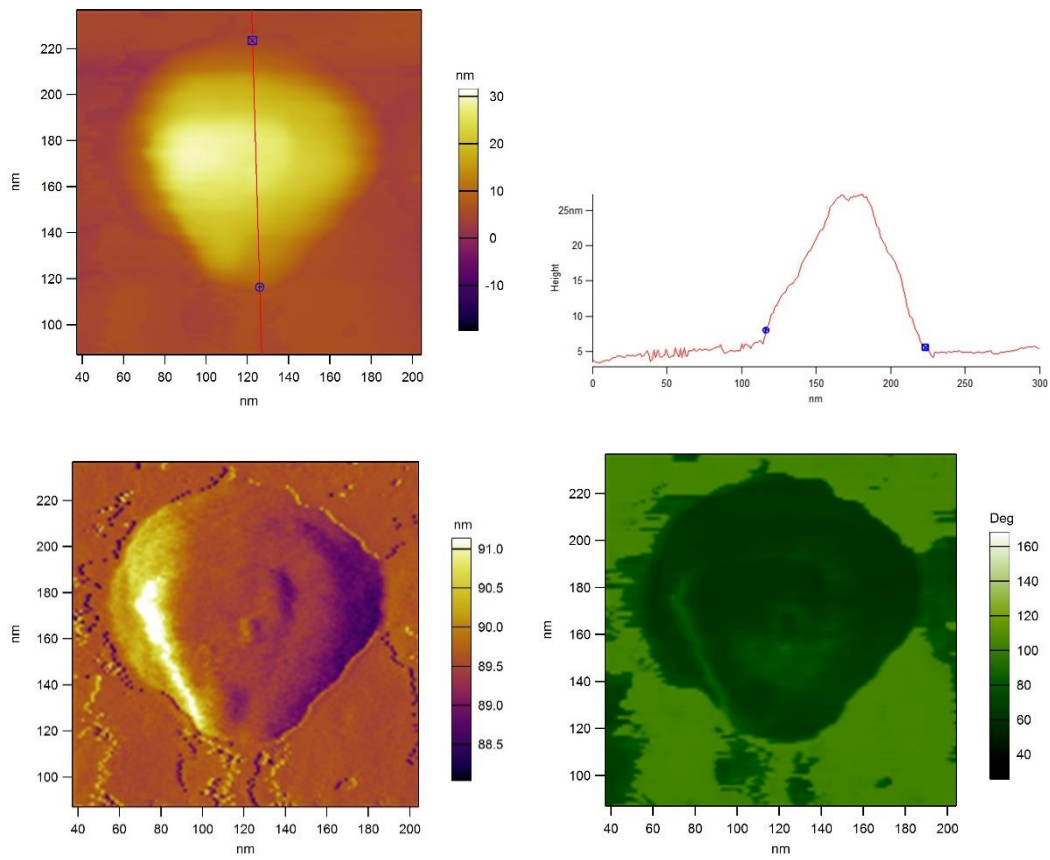
A20017: Height distribution: 4.02 ± 1.18 nm



A20018: Height distribution: 5.3 ± 1.19 nm



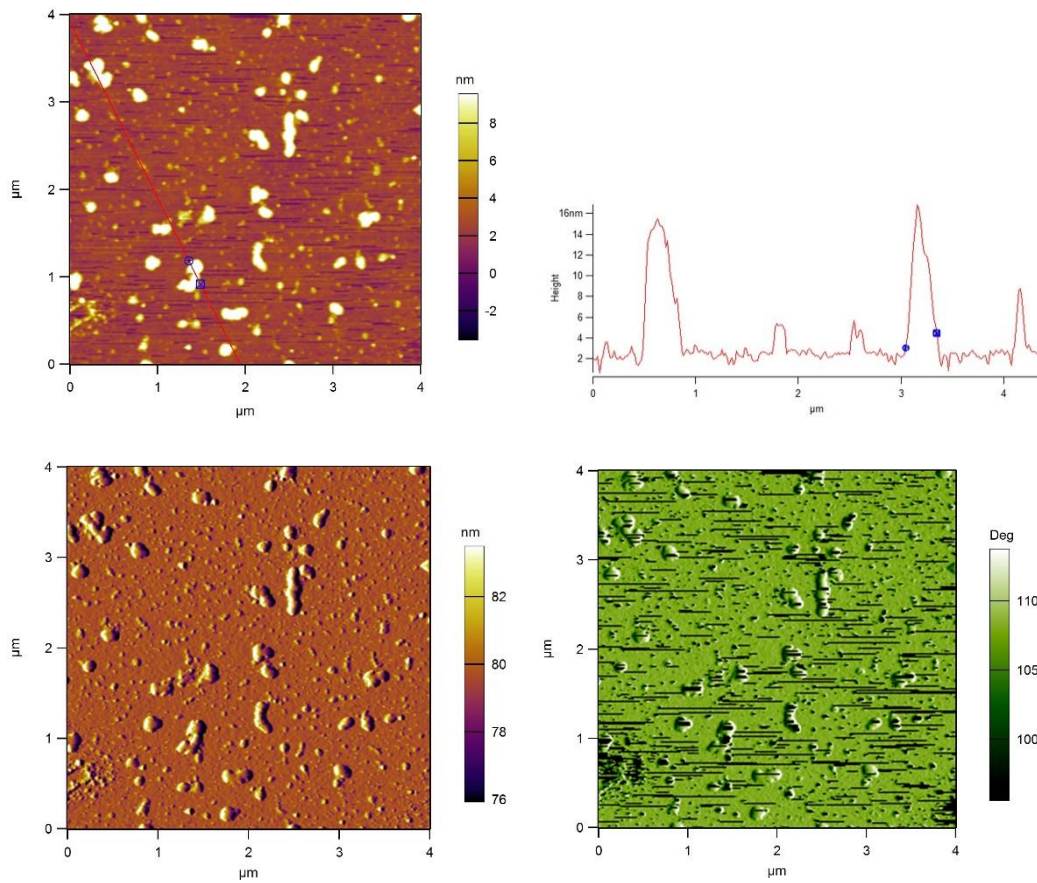
A20023: Height distribution: 4.64 ± 1.07 nm



Sample B

(Complex of PAA-PAM at pH 2 – 0.5 mg ml⁻¹ component concentration)

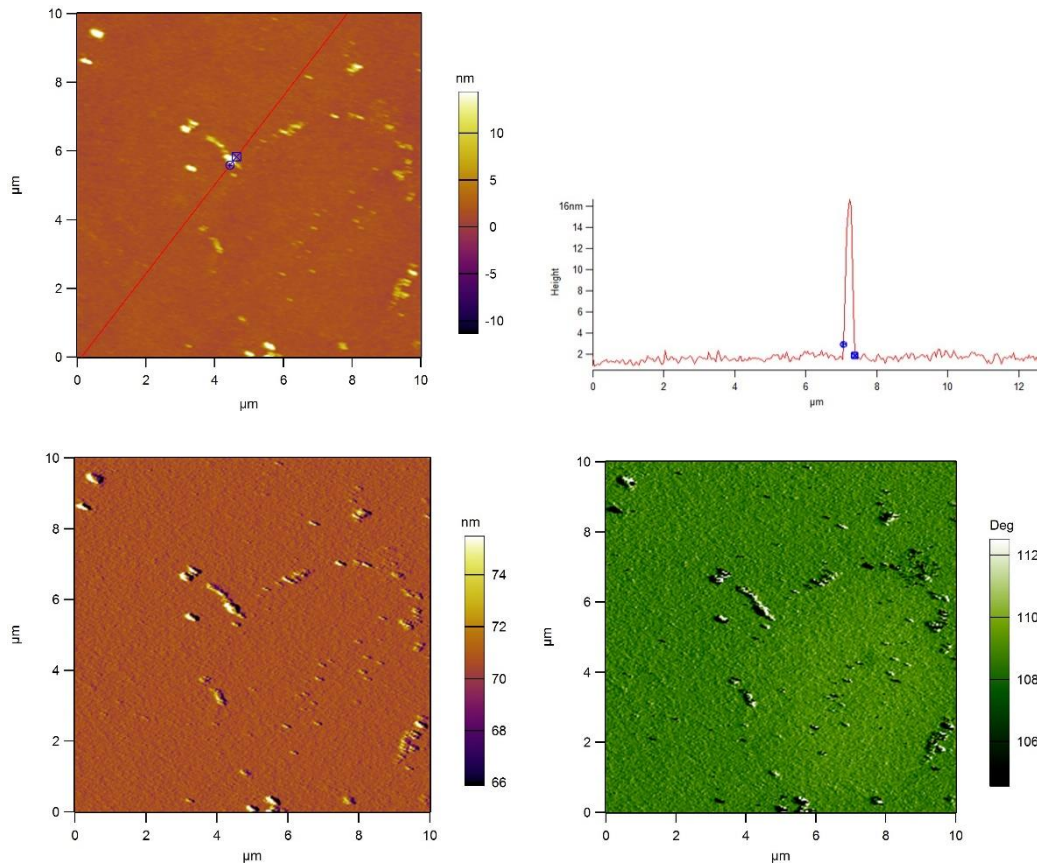
B20001: Height distribution: 2.4±0.33 nm



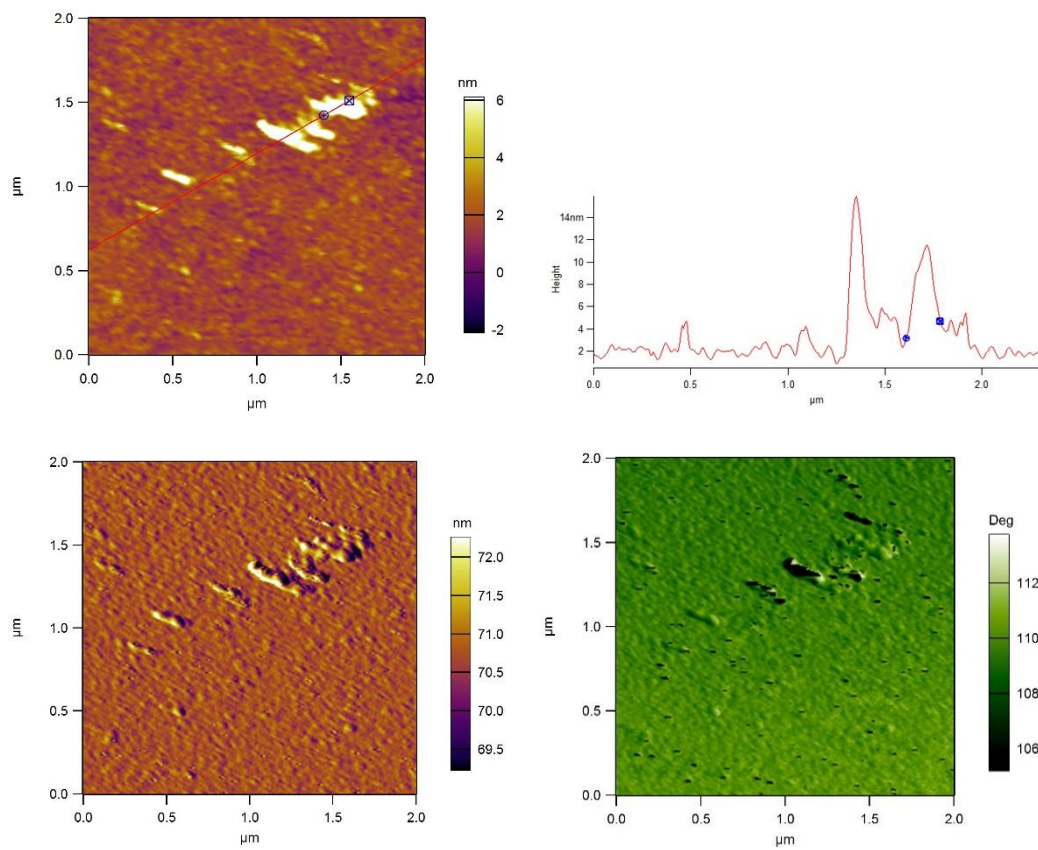
Sample C

PAA at 0.1 mg ml⁻¹ concentration.

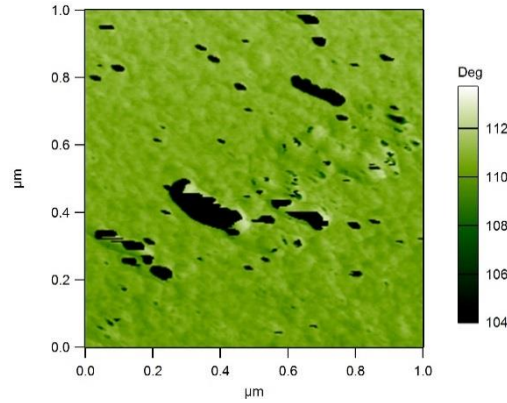
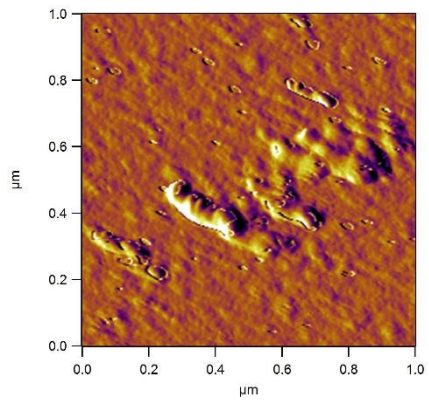
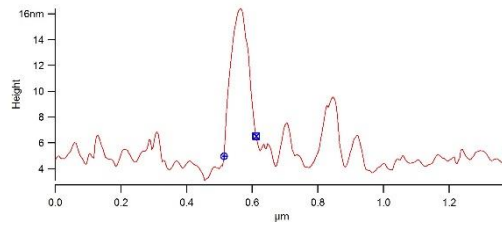
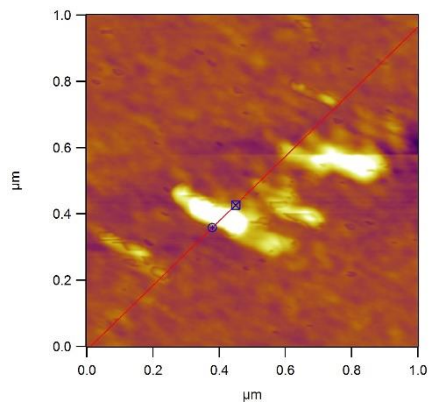
C20001: Height distribution: 1.56±0.36 nm



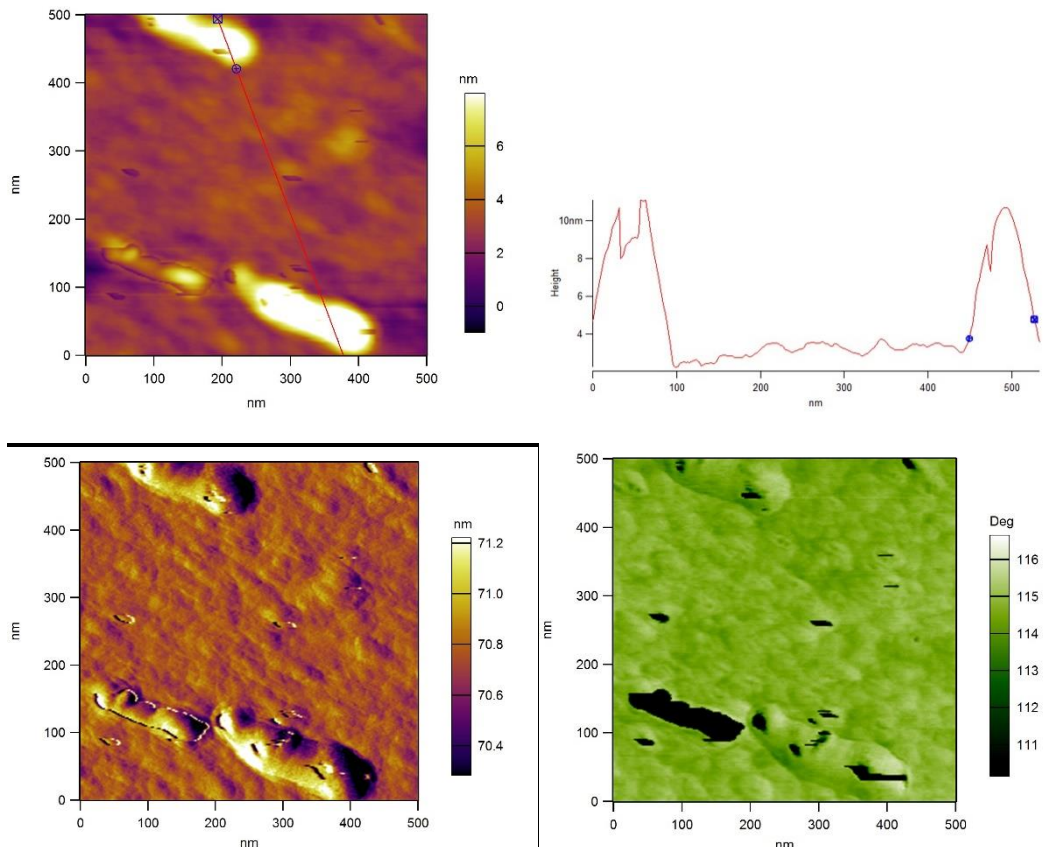
C20003: Height distribution: 1.77 ± 0.41 nm



C20004: Height distribution: 4.6 ± 0.48 nm



C20010: Height distribution: 2.88 ± 0.45 nm



Exemplary AFM height images (*top left*), height profile determined along the cross line section of height image (*top right*), amplitude image (*bottom left*) and phase tapping mode image (*bottom right*) obtained in the three samples for scan sizes ranging between $10 \times 10 \mu\text{m}^2$ to $0.3 \times 0.3 \mu\text{m}^2$.

AFM Summary:

It is difficult to determine any difference in sample height however the difference between the distinct globular particles in samples A and B compared to the full coating of the glass slide in sample C is apparent.

ALL images at full resolution are contained in an attached zip folder.

Energy Lost in Fluorescence – Stokes Shift

The emission of fluorescence labels in solution is highly dependent on the choice of solvent, as fluorescence quenching is a large concern in unregulated media. The fluorescent label ACE was studied at very low concentrations in order to minimize excimer formation which would form an additional degree of quenching. In dioxane however ACE shows a typical excitation / emission peaks of 295 nm and 340 nm which is consistent with prior research (Figure S12).

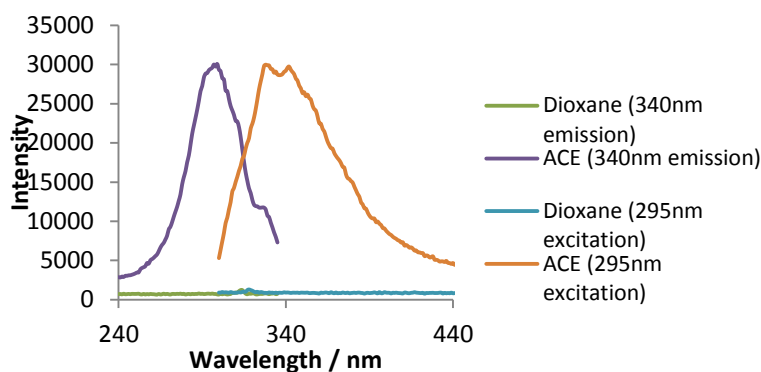


Figure S16– Excitation / Emission spectra of ACE label in dioxane (10^{-6} M)
Stokes Shift ($\Delta\nu$) = 32 nm

The presence and identification of fluorescent peaks in labelled polymers can be determined via steady state spectroscopy, comparing the emission and excitation spectra which are usually rough mirror images of one another. ACE-labelled poly(acrylamide) shows a peak excitation at 290 nm and an emission at 340 (Figure S13), consistent with the ACE fluorophore in solution. Unlabelled poly(acrylamide), bereft of aromatic groups or other conjugated double bonds, does not fluoresce in this region.

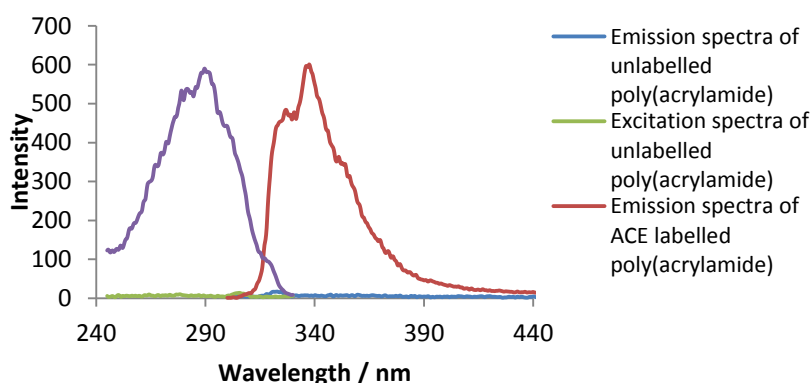


Figure S17 - Emission and Excitation Spectra of ACE labelled PAM solutions
Stokes Shift ($\Delta\nu$) = 48 nm

Comparison of SI12 with SI10 shows increased separation between the excitation and emission spectra of the excited label when attached to the PAM polymer backbone. The same is observed when ACE or AMMA is attached to PAA (see S14 and Fig. 1). Conversely calculating the Stokes shift for AMMA is complicated due to multiple absorbance / emission peaks between 350 and 400 nm.

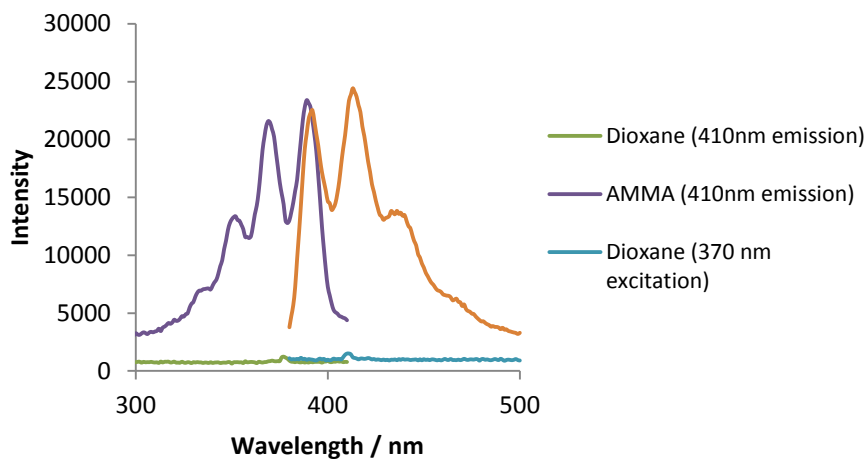


Figure S18 - Excitation / Emission spectra of AMMA label in dioxane (10^{-6} M)
Stokes Shift ($\Delta\nu$) = 2 nm

Summary:

When bound to a polymer backbone the ACE label demonstrates a significant loss of energy between absorption of a photon and emission, particularly in consideration of the fact it is absorbing in the ultraviolet region. Comparing the excitation and emission spectrum of ACE using only the peak wavelengths with a low band gap there is almost no overlap between the two spectra (Stokes Shift, $\Delta\nu = 45$ nm, spectral overlap 305-325 nm) whereas examination of the free label in dioxane with the same parameters shows much greater overlap ($\Delta\nu = 32$ nm, overlap 300 – 335 nm, see ESI). This indicates the fluorophore as a small molecular loses much less energy during the fluorescence process. Whilst the difference in solvent may have an effect this does imply at least some energy is being lost due to the presence of the polymer chain, possibly as vibrational energy along the chain. Conversely AMMA, whose structure means the label is much more loosely attached to the polymer backbone, the Stokes shift does not alter between the fluorophore in solution and after polymerization.

Fluorescence Energy Transfer Efficiency

The efficiency of energy transfer measurements can be represented via several methods³⁻⁴.

The efficiencies of Energy Transfer measurements between naphthalene and anthracene have previously been carried out on chain-end labelled poly(methacrylic acid) species³ which demonstrated an energy transfer efficiency that varied between 80 – 2 % depending on the conformational arrangement of the polymer.

These measurements were recreated using our dual labelled PAA and are shown below, with %E calculated using the following equation,

$$\%E = \frac{I_{Af}^R(\lambda_1) - (1 - 10^{-A(\lambda_2)})}{I_{Af}^R(\lambda_2) - (1 - 10^{-A(\lambda_1)})}$$

where $\lambda_1 = 391$ nm (wavelength at which only acceptor absorbs), $\lambda_2 = 333$ nm (wavelength at which only donor absorbs). As the ratio of AMMA exceeds that of ACE, and the ACE donor does not absorb at 391 nm, additional terms P and T used in previous studies³ have been discounted.

Using this equation it was seen that the energy transfer efficiency of P(AA-co-ACE-co-AMMA) varied between 15 and 77 % as the pH of the solution was adjusted (Fig. S19)

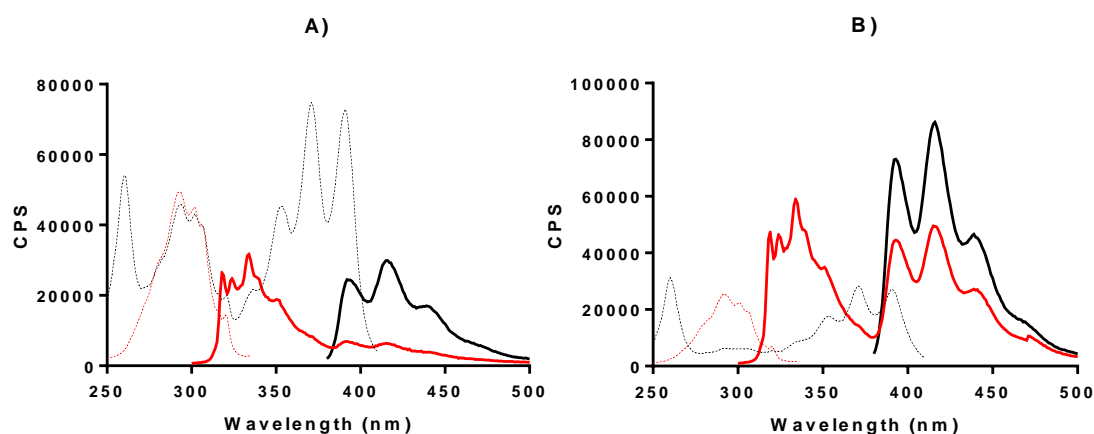


Figure S19 – Excitation (dashed lines) & Emission Measurements (solid lines) of P(AA-co-ACE-co-AMMA) (0.5 mg ml^{-1}) at pH 9 (A) and 3 (B), focusing on donor (red) and acceptor (black) chromophores

Fitting Fluorescence Lifetimes

Data shown in the manuscript is calculated by fitting fluorescence lifetimes to dual exponential fits. This is done to provide more accurate representation of the fluorophore excited state decay, particularly around the initial pulse. The fits are carried out using 2 different equations:

$$\text{Single decay: } I(t) = A + I_0 \exp\left(\frac{-t}{\tau_f}\right)$$

$$\text{Dual Decay: } I(t) = A + B_1 \exp\left(\frac{-t}{\tau_{f1}}\right) + B_2 \exp\left(\frac{-t}{\tau_{f2}}\right)$$

In the dual decay the combined lifetime is shown as

$$\tau = \frac{B_1 \tau_{f1}^2 + B_2 \tau_{f2}^2}{B_1 \tau_{f1} + B_2 \tau_{f2}}$$

Comparing the decay of P(AA-co-ACE) the difference can be shown in Fig. S25 – 27. Fig. S25 - S26 show that though both fits follow the fluorescence decay well there is tighter accuracy with the dual model, particularly immediately following the pulse and at the tail end of the decay.

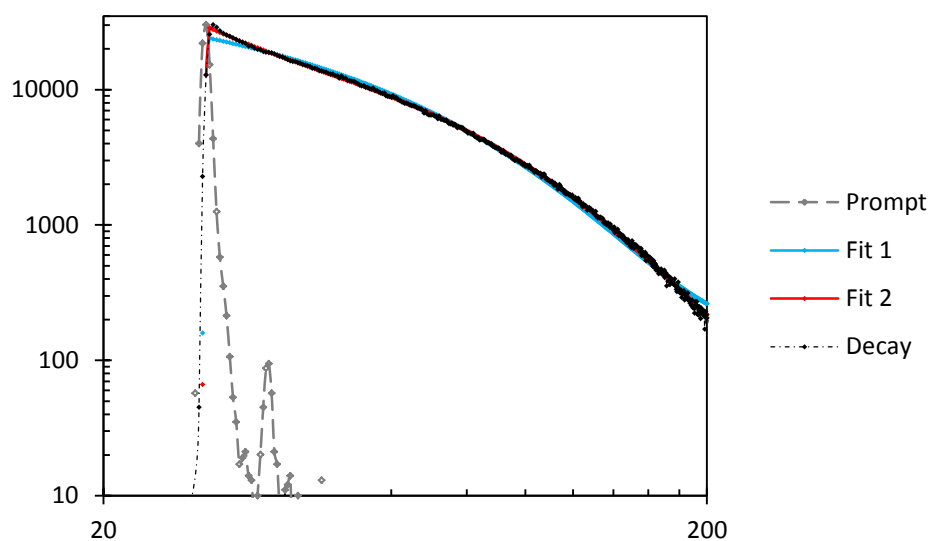


Fig. S25 – Fluorescence decay (-) of P(AA-co-ACE) at pH 3.9. A silica prompt is used to model the excitation light pulse (grey line) and two fitting models (single = blue, dual = red).

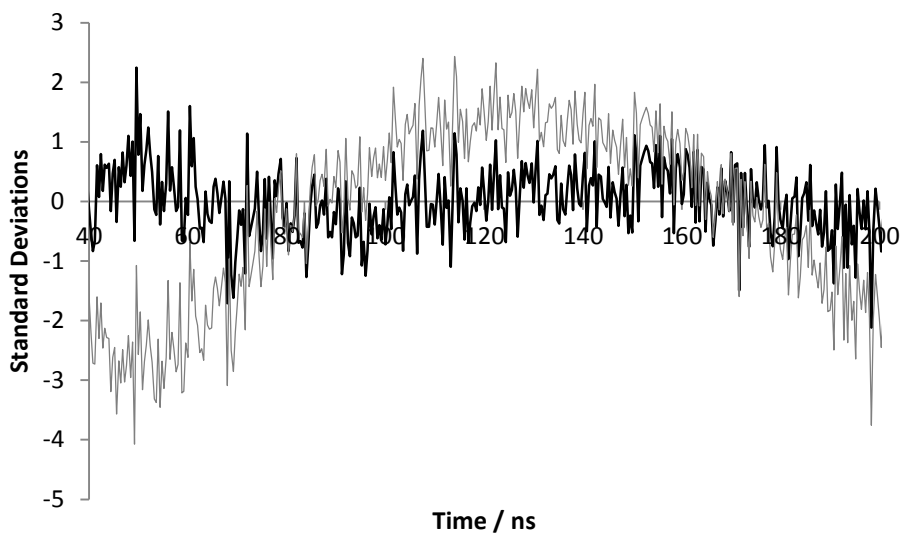


Fig. S26 - Residual standard deviations of the fit to fluorescence decay curves.

When the lifetimes from both of these are plotted they show similar results – however only the dual lifetimes are reported in the final manuscript.

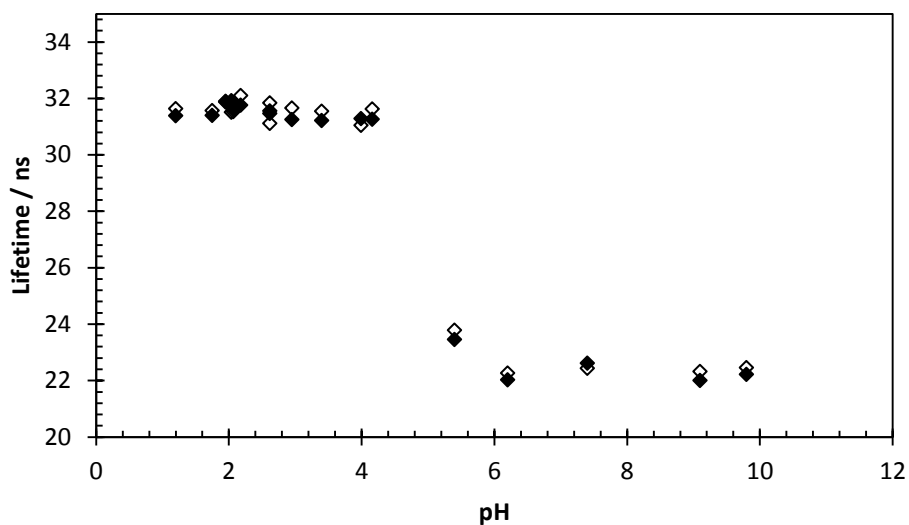


Figure S27 - The lifetime of P(AA-co-ACE) fitted with a single (◇) and double (◆) exponential decay.

E_{DT} of Dual Labels along Polymer Chain

It is stated in the paper that when the dual labelled polymer P(AA-co-ACE-co-AMMA) complexes with PAM, accompanying an increase in E_{ST} from 0.44 to 0.7 there is also a 40% increase in E_{DT} from 0.05 to 0.07. The raw lifetime values for this statement are now shown in the publication and are included here as evidence.

Table S3. Average lifetimes of experiments:

	< pH 3	3.5 < pH < 5	> pH 6
PAA ACE	31.62 ± 0.29	31.22 ± 0.35	22.52 ± 0.66
PAA-ACE-AMMA	29.99 ± 0.14	29.68 ± 0.65	23.40 ± 0.66
PAA-ACE-AMMA + PAM	29.32 ± 0.04	29.26 ± 0.88	23.50 ± 0.98

Table S4. E_{DT} of

	< pH 3	3.5 < pH < 5	> pH 6
PAA-ACE-AMMA	0.051	0.062	-0.004
PAA-ACE-AMMA + PAM	0.073	0.075	-0.004

Table S5 – Distance in nm

	< pH 3	3.5 < pH < 5	> pH 6
PAA-ACE-AMMA	2.61	2.53	> 5
PAA-ACE-AMMA + PAM	2.46	2.44	> 5

$E_{D\tau}$ of Single Labels along Multiple Chains

Raw fluorescence decay curves of the PAA-co-ACE are shown below:

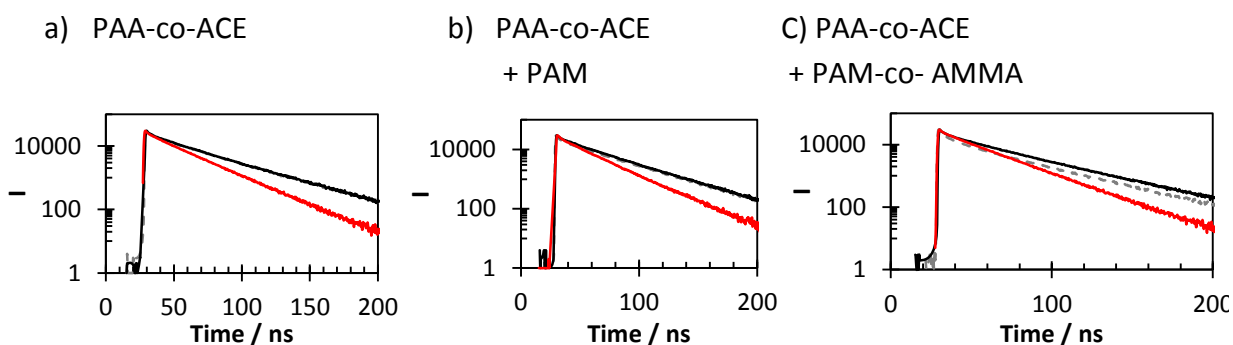


Fig S28 – Raw fluorescence decay curves of P(AA-co-ACE) with and without PAM.

Decays at pH 2 = dotted grey, at pH 4 = black, at pH 7 = red.

Condition	pH 2	pH 4	pH 7
a) PAA-co-ACE	T = 31.9 ns, SD = 0.16 ns, CHISQ = 1.81	T = 31.8 ns, SD = 0.151 ns, CHISQ = 1.70	T = 22.4 ns, SD = 0.272 ns, CHISQ = 1.71
b) PAA-co-ACE + PAM	T = 31.9 ns, SD = 0.99 ns, CHISQ = 2.04	T = 31.8 ns, SD = 0.174 ns, CHISQ = 1.70	T = 23.2 ns, SD = 0.752 ns, CHISQ = 2.05
c) PAA-co-ACE + PAM-co-AMMA	T = 26.9 ns, SD = 0.36 ns, CHISQ = 1.61	T = 31.2 ns, SD = 0.929 ns, CHISQ = 2.40	T = 23.2 ns, SD = 0.752 ns, CHISQ = 1.09

When collated these fits were used to create Fig. S28.

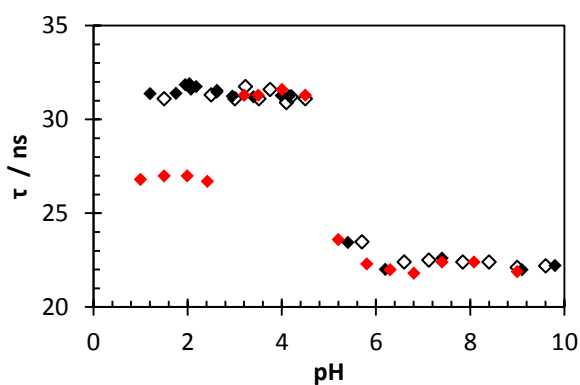


Fig. 14 recreated.

From the data shown in Fig. 13 it can be seen that there is a large difference in the E_{DT} of singly labelled PAA-ACE with PAM-AMMA, but not with PAM.

Table S6. Average lifetimes of experiments:

	< pH 3	3.5 < pH < 5	> pH 6
PAA ACE	31.62 ± 0.29	31.22 ± 0.35	22.52 ± 0.66
+ PAM	31.31 ± 0.12	31.23 ± 0.35	22.50 ± 0.45
+ PAM-ACE	26.87 ± 0.15	31.38 ± 0.15	22.34 ± 0.82

Table S7. E_{DT} of

	< pH 3	3.5 < pH < 5	> pH 6
+ PAM	0.0096	0.0005	0.0008
+ PAM-ACE	0.1500	-0.0041	0.0078

Table S8. Distance in nm between Labels

	< pH 3	3.5 < pH < 5	> pH 6
+ PAM	>5	>5	>5
+ PAM-ACE	2.16	>5	>5

E_{ST} of Single Labels Across Multiple Polymer Chains

It is stated in the paper that when the singly labelled polymer P(AA-co-ACE) complexes with P(AM-co-AMMA), accompanying an increase in E_{DT} shown in the paper there is evidence of E_{ST} to accompany it. As the distinct AMMA peaks at 400 nm are not discernible this raw data was not attached to the full manuscript but is shown below in Fig. S29.

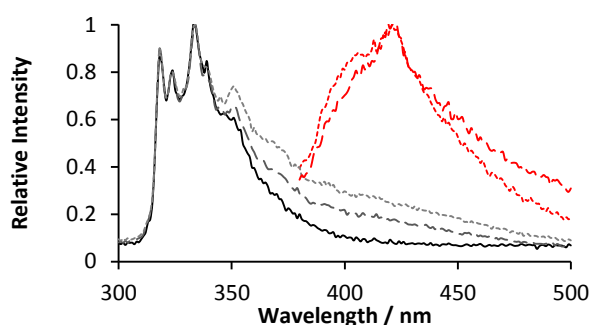


Figure S29. Emission spectra (relative to peak emission at 333 / 420 nm) of singly labelled polymers P(AA-co-ACE) (solid black line) (1 mg ml^{-1}) with P(AM-co-AMMA) (1 mg ml^{-1} – dashed line, 2 mg ml^{-1} – dotted line). In black $\lambda_{ex} = 290 \text{ nm}$, excitation of ACE leading to potential energy transfer to AMMA. In red $\lambda_{ex} = 370 \text{ nm}$, direct excitation of AMMA.

The emission of P(AA-co-ACE) shows the single fluorophore has no emission in the 400 nm region. Addition of P(AM-co-AMMA) however gives a broad band emission in this region that doubles at higher concentrations. Furthermore the dynamics of the AMMA probe have not been affected by the proximity to the P(AA-co-ACE) as direct excitation of this acceptor FRET probe show it still has the same emission profile regardless of the mixture.

Table S9. E_{ST} of P(AA-co-ACE) alone (no FRET recorded, compared as a baseline reading) with equivalent and double PAM concentration.

	< pH 3	3.5 < pH < 5	> pH 6
PAA -ACE	0.01	0.00	0.00
+ PAM	0.19	0.00	0.00
+ PAM x 2	0.28	0.00	0.00

Full Details of Fig. 13 and 14

The Chisquared (χ^2) (degrees of Freedom) and data entries for fluorescence lifetimes as shown in Fig. 13 and 14 are shown in the tables below. All data was recorded on an Edinburg 199 instrument with a time calibration of 0.4 nanoseconds per channel. Data was recorded across 512 channels with the fluorescence data fitted across the decay from channels 70 to 512. Fluorescence excitation was always 295 nm and emission 350 nm.

The combined lifetime and sd. Deviations of fits from the dual exponential decays were calculated using the following equations:

The lifetime of

$$I = A \exp(-t / \tau_1) + B \exp(-t / \tau_2)$$

is given by

$$\langle \tau \rangle = \frac{A\tau_1^2 + B\tau_2^2}{A\tau_1 + B\tau_2}$$

The error, σ , in τ comes from the standard equation

$$\sigma^2 = \left(\frac{\partial \langle \tau \rangle}{\partial \tau_1} \right)^2 (\Delta \tau_1)^2 + \left(\frac{\partial \langle \tau \rangle}{\partial \tau_2} \right)^2 (\Delta \tau_2)^2$$

which means that

$$\sigma = \frac{1}{A\tau_1 + B\tau_2} \sqrt{A^2 (\Delta \tau_1)^2 (2\tau_1 - \langle \tau \rangle)^2 + B^2 (\Delta \tau_2)^2 (2\tau_2 - \langle \tau \rangle)^2}$$

Table S10 - Raw Data for Fig. 13

Sample	pH	Lifetime	Std. Dev	B1	B2	A	ChiSq
PAA	1.2	31.4	0.43	0.24	1.0	119.6	1.73
PAA	1.75	31.4	0.77	0.22	0.9	138.4	1.71
PAA	1.95	31.9	0.63	0.24	1.0	151.4	1.26
PAA	2.04	31.9	0.62	0.30	1.2	152.8	1.30
PAA	2.07	31.6	0.52	0.37	1.5	127.0	2.57
PAA	2.18	31.8	0.59	0.18	0.7	149.8	2.85
PAA	2.62	31.6	0.61	0.20	0.8	131.0	1.28
PAA	2.62	31.5	0.36	0.32	1.3	97.2	1.17
PAA	2.95	31.5	0.54	0.30	1.2	118.6	1.07
PAA	3.4	31.6	0.65	0.10	0.4	153.0	1.30
PAA	3.99	31.7	0.67	0.15	0.6	148.2	1.40
PAA	4.16	31.7	0.61	0.16	0.6	143.2	1.24
PAA	5.4	23.4	0.27	0.74	2.9	120.4	2.23
PAA	6.2	23.0	0.26	0.17	0.7	126.3	1.44

PAA	7.4	22.6	0.23	0.17	0.7	117.0	1.37
PAA	9.1	23.0	0.54	0.28	1.1	132.0	1.68
PAA	9.8	22.2	0.51	0.26	1.0	132.0	1.55
PAA*	1.18	30.0	0.35	0.7421	0.351	80.122	1.04
PAA*	1.9	30.1	0.13	0.22	0.179	70.881	1.04
PAA*	2.45	29.9	0.21	0.111	0.356	21.27	1.01
PAA*	3.3	30.0	0.14	0.08403	0.246	77.42	1.00
PAA*	4.19	29.5	0.14	0.166	0.258	55.12	1.00
PAA*	4.71	29.5	0.18	0.138	0.298	30.01	1.00
PAA*	4.82	29.4	0.11	0.192	0.235	74.04	1.00
PAA*	5.1	27.6	0.17	0.117	0.303	40.11	1.13
PAA*	5.96	24.8	0.13	0.278	0.7531	52.23	1.13
PAA*	6.25	24.4	0.31	0.148	0.646	25.5	1.73
PAA*	6.31	23.1	0.18	0.2761	0.3209	53.41	1.13
PAA*	6.86	23.6	1.06	0.116	0.279	16.63	1.78
PAA*	8	23.1	0.07	0.831	0.137	77.6	1.78
PAA*	9.24	23.5	0.17	0.312	1.23	64.09	1.78
PAA*	9.46	22.9	0.14	0.793	0.622	82.77	1.78
PAA*	9.94	23.1	0.25	6.771	0.278	17.19	1.78
PAA*	9.98	23.5	0.12	0.273	5.612	26.62	1.78
PAA*-PAM	1.67	29.3	0.34	0.108	0.331	13.9	1.56
PAA*-PAM	2.35	29.3	0.25	0.151	0.315	11.7	1.50
PAA*-PAM	3.2	29.3	0.19	0.142	0.294	25.8	1.78
PAA*-PAM	3.9	29.3	0.24	0.08	0.341	47.9	1.57
PAA*-PAM	4.1	29.1	0.20	0.159	0.348	63.0	1.56
PAA*-PAM	4.5	28.1	0.36	0.113	0.407	56.6	1.56
PAA*-PAM	5.6	25.9	0.33	0.104	0.435	76.7	1.57
PAA*-PAM	5.6	26.5	0.26	0.125	0.302	58.1	2.67
PAA*-PAM	5.79	24.2	0.17	9.433	0.329	66.3	1.70
PAA*-PAM	5.9	25.7	0.50	7.694	0.301	77.9	1.57
PAA*-PAM	7	23.7	0.23	0.121	0.288	66.8	1.49
PAA*-PAM	8.2	23.5	0.14	0.207	0.217	39.3	1.57
PAA*-PAM	9.19	23.2	0.22	0.161	0.361	69.8	1.13
PAA*-PAM	9.86	23.5	0.19	0.143	0.279	23.8	1.70

Table S11 - Raw Data for Fig. 14

Sample	pH	Lifetime	Std. Dev	B1	B2	A	ChiSq
PAA	4.80	29.17	0.49	0.25	0.98	89.51	1.09
PAA	7.84	22.41	0.27	0.74	2.94	12.42	1.78
PAA	3.75	30.62	0.42	0.25	1.01	112.00	1.51
PAA	3.23	30.77	0.46	0.27	1.08	37.34	1.09
PAA	2.83	31.28	0.30	0.31	1.26	98.06	1.74

PAA	6.60	23.45	0.26	0.17	0.69	26.25	1.15
PAA	9.58	23.25	0.23	0.17	0.66	16.99	1.10
PAA	3.77	31.16	0.38	0.21	0.83	112.70	1.21
PAA	2.87	31.14	0.43	0.18	0.72	118.00	1.40
PAA	1.53	31.12	0.43	0.18	0.73	116.40	1.43
PAA	3.51	31.09	0.48	0.14	0.54	126.10	1.74
PAA	2.36	31.08	0.48	0.08	0.31	125.30	1.77
PAA - PAM	2.95	32.04	0.43	0.24	0.96	119.60	1.39
PAA - PAM	1.20	31.08	0.77	0.22	0.89	138.40	2.27
PAA - PAM	1.95	31.86	0.63	0.24	0.96	151.40	2.52
PAA - PAM	3.40	31.61	0.62	0.30	1.18	152.80	2.59
PAA - PAM	3.99	31.88	0.52	0.37	1.46	127.00	2.05
PAA - PAM	2.62	31.56	0.59	0.18	0.73	149.80	2.28
PAA - PAM	2.62	31.16	0.61	0.20	0.79	131.00	2.55
PAA - PAM	2.07	31.61	0.36	0.32	1.29	97.18	2.34
PAA - PAM	4.16	31.95	0.54	2.30	9.18	118.60	2.15
PAA - PAM	2.18	31.76	0.65	0.10	0.39	153.00	2.61
PAA - PAM	1.75	31.40	0.67	0.15	0.62	148.20	2.80
PAA - PAM	2.04	31.91	0.61	0.16	0.64	143.20	2.48
PAA - PAM	7.40	22.41	0.27	0.74	2.94	12.42	1.78
PAA - PAM	5.40	23.45	0.26	0.17	0.69	26.25	1.15
PAA - PAM	9.10	22.21	0.23	0.17	0.66	16.99	1.10
PAA-PAM*	3.93	31.22	0.61	0.60	2.40	158.90	1.21
PAA-PAM*	2.42	26.70	1.01	0.09	0.36	134.80	2.30
PAA-PAM*	1.99	26.96	0.90	0.16	0.65	153.30	2.06
PAA-PAM*	6.80	21.32	0.21	0.35	1.42	339.10	1.13
PAA-PAM*	8.08	21.43	0.64	2.36	9.43	342.60	4.25
PAA-PAM*	4.28	30.95	0.39	10.72	42.90	102.90	1.54
PAA-PAM*	3.30	31.31	0.41	0.16	0.66	110.80	1.32
PAA-PAM*	1.50	26.83	0.41	4.48	17.91	261.53	2.31
PAA-PAM*	9.00	21.63	0.48	4.42	17.66	185.43	2.37

References in ESI

1. Swift, T.; Swanson, L.; Geoghegan, M.; Rimmer, S., The pH-responsive behaviour of poly(acrylic acid) in aqueous solution is dependent on molar mass. *Soft Matter* **2016**, (12), 2542 - 2549.
2. Chang, C.; Muccio, D. D.; St. Pierre, T., Determination of the tacticity and analysis of the pH titration of poly(acrylic acid) by proton and carbon-13 NMR. *Macromolecules* **1985**, 18 (11), 2154-2157.
3. Liu, G.; Guillet, J.; Al-Takrity, E. T. B.; Jenkins, A.; Walton, D., Dimensions of polyelectrolytes using the " spectroscopic ruler". 2. Conformational changes of poly (methacrylic acid) chains with variation in pH. *Macromolecules* **1991**, 24 (1), 68-74.
4. Ruiz-Pérez, L.; Pryke, A.; Sommer, M.; Battaglia, G.; Soutar, I.; Swanson, L.; Geoghegan, M., Conformation of Poly(methacrylic acid) Chains in Dilute Aqueous Solution. *Macromolecules* **2008**, 41 (6), 2203-2211.